

## A modeling study of aqueous production of dicarboxylic acids: 1. Chemical pathways and speciated organic mass production

Barbara Ervens,<sup>1</sup> Graham Feingold,<sup>2</sup> Gregory J. Frost,<sup>3,4</sup> and Sonia M. Kreidenweis<sup>5</sup>

Received 25 November 2003; revised 21 May 2004; accepted 10 June 2004; published 12 August 2004.

[1] While the formation pathways and thermodynamic properties of inorganic species (e.g., sulphate) in atmospheric aerosols are well understood, many more uncertainties exist about organics. In the present study we present oxidation pathways of organic gas phase species that lead to low volatility organic compounds (C<sub>2</sub>-C<sub>6</sub> dicarboxylic acids, pyruvic acid) in both the aqueous and gas phases. This mechanism is implemented in a cloud parcel model initialized with pure (NH<sub>4</sub>)<sub>2</sub>SO<sub>4</sub> particles in 10 discrete sizes. Under clean continental conditions a few cloud processing cycles produce a total organic mass addition of ~150 ng m<sup>-3</sup>. Individual resuspended aerosol size classes contain significant organic fractions, sometimes higher than 50%. These are likely upper bound estimates of organic mass production. In a polluted, i.e., SO<sub>2</sub>-rich scenario, about 400 ng m<sup>-3</sup> organic material is produced after about eight cloud cycles. Since the initial conditions in this latter case favor significant production of sulphate, the organic fraction of the aerosol mass after cloud processing represents a much lower percentage of the total aerosol mass. Oxalic, glutaric, adipic, and pyruvic acids are the main contributors to the organic fraction in both cases. In agreement with observations, the oxalate fraction in processed particles exceeds the fractions of other dicarboxylic acids since it represents an end product in the oxidation of several organic gas phase species. The study suggests that cloud processing may act as a significant source of small dicarboxylic acids, some fraction of which can be retained in the aerosol phase upon drop evaporation. *INDEX TERMS*: 0305 Atmospheric Composition and Structure: Aerosols and particles (0345, 4801); 0320 Atmospheric Composition and Structure: Cloud physics and chemistry; 0365 Atmospheric Composition and Structure: Troposphere—composition and chemistry; *KEYWORDS*: dicarboxylic acids, hygroscopicity, organic aerosols

**Citation:** Ervens, B., G. Feingold, G. J. Frost, and S. M. Kreidenweis (2004), A modeling study of aqueous production of dicarboxylic acids: 1. Chemical pathways and speciated organic mass production, *J. Geophys. Res.*, 109, D15205, doi:10.1029/2003JD004387.

### 1. Introduction

[2] Many uncertainties exist in estimating the impact of aerosol particles on climate. Besides the direct effect of aerosols on radiation, their indirect effect, i.e., the interaction between aerosol particles and clouds has yet to be quantified. Several studies have shown that the production of sulphate in cloud drops can contribute significantly to the aerosol mass [e.g., Chameides and Stelson, 1992; Hegg *et al.*, 1996; Zhang *et al.*, 1999] and may lead either to an enhancement or to a suppression of the cloud drop number

concentration [Feingold and Kreidenweis, 2000, 2002]. This mass addition by aqueous phase processes influences the resulting aerosol size distribution, which in turn might lead to a modified drop size distribution in subsequent clouds.

[3] While previous studies have focused on the inorganic content of aerosols (in particular sulphate), the chemical composition of secondary aerosols is usually much more complex and may include hundreds of different organic compounds (including alkanes, carboxylic acids and aldehydes) [e.g., Rogge *et al.*, 1996]. The study by Saxena and Hildemann [1996] shows that the organic fraction of fresh anthropogenic aerosols consists mainly of less oxidized organics (e.g., alkanes) and is rather hydrophobic. They find that aged and secondary particles are more hygroscopic with an enhanced fraction of oxygenated organics, e.g., dicarboxylic acids which can contribute up to 50% of the organic aerosol mass [Satsumbayashi *et al.*, 1989].

[4] Single particle analyses by Lee *et al.* [2002, 2003] from the Atlanta Supersite Project illustrate that in clean continental air more than 70% of all particles are internal mixtures of sulphate and organics. Aerosols containing

<sup>1</sup>Cooperative Institute for Research in the Atmosphere, Colorado State University, Fort Collins, Colorado, USA.

<sup>2</sup>Environmental Technology Laboratory, NOAA, Boulder, Colorado, USA.

<sup>3</sup>Aeronomy Laboratory, NOAA, Boulder, Colorado, USA.

<sup>4</sup>Cooperative Institute for Research in Environmental Sciences, University of Colorado, Boulder, Colorado, USA.

<sup>5</sup>Atmospheric Science Department, Colorado State University, Fort Collins, Colorado, USA.

compounds which are formed mainly by direct gas phase precursors, e.g., nitrate, do not exhibit such high organic fractions. It is well established that globally the major fraction (up to 84%) of sulphate is formed within clouds [Langner and Rodhe, 1991; Wojcik and Chang, 1997]. Hydroxymethanesulfonate ( $\text{HMS}^-$ ), the adduct of formaldehyde and sulphur(IV), is exclusively formed in the aqueous phase, so its presence in particles is an additional tracer for processing by aqueous phase chemistry [Dixon and Aasen, 1999; Whiteaker and Prather, 2003]. Since  $\text{HMS}^-$  was found in the same particles analyzed by Lee et al. [2002, 2003], it was assumed that the high amounts of dicarboxylic acids in these particles also originated exclusively from chemical processes in cloud water.

[5] Existing detailed chemical schemes describe the gas phase formation processes of oxygenated organic compounds, which are possible precursors for dicarboxylic acids [e.g., Pun et al., 2000; Griffin et al., 2002]. It is likely that long chain dicarboxylic acids ( $>C_6$ ) are formed from naturally-occurring fatty acids, while the precursors for smaller dicarboxylic acids ( $\leq C_6$ ) may be alkenes, aldehydes or other less oxygenated organics. It has also been suggested that small dicarboxylic acids might be formed by the decay of longer acids [Kawamura and Sakaguchi, 1999]. While gas phase oxidation of organics usually leads to shorter carbon chains, in the aqueous phase the carbon chains remain intact for a longer time.

[6] Jang and Kamens [2001] showed that low volatility constituents of secondary organic aerosols are formed by heterogeneous processes, but their study is restricted to formation on very acidic sulphuric acid aerosols. In addition to gas or aqueous phase processes, the oxidation of hydrophobic films on aerosol surfaces might lead to oxalic and glyoxylic acid [Eliaison et al., 2003]. While the timescale of this oxidation process is of interest for the activation process of coated particles, the mass of a processed monolayer film will not contribute significantly to the total aerosol mass. The impact of aqueous phase processes on the formation of low-volatility organic compounds has been suggested in the recent literature [Chebbi and Carlier, 1996; Blando and Turpin, 2000]. Anttila and Kerminen [2003] estimated that such processes will contribute significantly to particle growth in the very early stages of droplet formation. However, few current chemical models describe the formation pathways of di- and ketocarboxylic acids by aqueous phase processes. Recently it has been suggested that in-cloud chemistry might contribute to the formation of oxalic acid initiated by the oxidation of aromatics [Ervens et al., 2003a] or ethylene and acetylene [Warneck, 2003].

[7] The possible impact of dicarboxylic acids in particles on the interactions between aerosols and cloud droplet formation has been investigated in several laboratory studies. Many recent studies show that the hygroscopic behavior of dicarboxylic acids in pure and/or internally mixed aerosols is significantly correlated with their solubility in water [e.g., Novakov and Penner, 1993; Shulman et al., 1996; Cruz and Pandis, 2000; Peng et al., 2001; Prenni et al., 2001; Raymond and Pandis, 2002; Brooks et al., 2002; Kumar et al., 2003]. Thus their efficiency as condensation nuclei may be estimated. The addition of moderately soluble or slightly soluble organic material to particles may also lead to a reduced droplet surface tension (Kelvin effect)

[Facchini et al., 1999], which also needs to be taken into account.

[8] Currently there is no comprehensive chemical multiphase mechanism including both the formation of organic aerosol mass and sulphate in clouds. The reason for this gap in model development might be the limited state of cloud chemistry mechanisms [Herrmann, 2003]. Currently the most detailed cloud chemistry mechanism is represented by CAPRAM (Chemical Aqueous Phase Radical Mechanism) [Herrmann et al., 2000; Ervens et al., 2003a] (<http://projects.tropos.de:8088/capram>), which considers organic compounds with one and two carbon atoms. In the current study, parts of the extended version of CAPRAM [Ervens, 2001] were combined with a newly compiled mechanism considering the oxidation and formation of even higher organics ( $\leq C_6$ ). This multiphase mechanism is applied to a cloud model with size-resolved particles to study possible effects of chemical processes in clouds with respect to the production of small dicarboxylic acids.

## 2. Model Description

[9] The cloud parcel model used in the current study is described in detail elsewhere [Feingold and Heymsfield, 1992; Feingold et al., 1998]; therefore we give only a brief description here. The model considers the growth of a population of aerosol particles by water vapor uptake in a rising parcel of air. The particle growth is solved on a moving mass grid for maximum accuracy and to retain full information on aerosol composition within droplets. In the current study, parcels are driven by prescribed trajectories that derive from a three-dimensional Eulerian cloud model [Stevens et al., 1996]. We consider a 12-hour simulation, with each hour of the cloud cycle repeating the same trajectory. Parameters such as relative humidity ( $\text{RH} > 80\%$ ), temperature ( $282 \text{ K} < T < 288 \text{ K}$ ), pressure ( $920 \text{ hPa} < p < 970 \text{ hPa}$ ), updraft velocity ( $10 \text{ cm s}^{-1} < w < 80 \text{ cm s}^{-1}$ ,  $10 \text{ cm s}^{-1} < |-w| < 110 \text{ cm s}^{-1}$ ), position of the air parcel ( $300 \text{ m} < h < 680 \text{ m}$ ), and cloud contact time always have the same values for each of the twelve one-hour cloud cycles. During each hour the parcel encounters a cloud for about 800 s. The mean and maximum liquid water mixing ratios are 0.19 and  $0.28 \text{ g kg}^{-1}$ , respectively.

[10] The dry aerosol size distribution is defined for ten logarithmically spaced size classes over the range  $0.013 \mu\text{m} < r < 1.2 \mu\text{m}$ . The initial size distribution is a lognormal function with a number concentration of  $500 \text{ cm}^{-3}$  or  $100 \text{ cm}^{-3}$  for polluted or clean continental conditions, respectively, a median radius of  $0.06 \mu\text{m}$ , and a geometric standard deviation of 1.6. We do not consider aerosol growth processes such as adsorption or coagulation, or loss processes such as deposition.

[11] The initial aerosol particles are composed of pure ammonium sulphate. Their hygroscopic growth is described using the Zdanovskii-Stokes-Robinson parameterization [Zdanovskii, 1948; Stokes and Robinson, 1966] for a variable ratio of ammonium to sulphate ions, consistent with ammonium sulphate, ammonium bisulphate and sulphuric acid. Gas uptake processes as well as chemical aqueous phase reactions occur in the model only if two conditions are met: (1) the total liquid water content is greater than  $1 \text{ mg kg}^{-1}$ , and (2) for each size class, the sum

of the sulphate and ammonium concentration does not exceed 1 M (i.e., corresponding to an ionic strength  $I$  of  $0.5 \text{ M} \leq I_{\text{max}} \leq 1 \text{ M}$  for an ammonium (bi-)sulphate solution). Due to the significant lack of appropriate data for the estimation of rate coefficients at higher ionic strengths (either based on experimental data or thermodynamic approaches [Pitzer, 1991; Herrmann, 2003]), we do not consider chemical aqueous phase processes at  $I > 1 \text{ M}$ .

[12] In addition, a maximum limit of an ionic strength of  $I = 1 \text{ M}$  for the application of the Henry's law constants might even be an overestimate of the impact of the aqueous phase as a sink, since it is known that the solubility of organic gases generally decreases with increasing ionic strength ('salting-out effect'). However, empirical correction parameters ('Setchenow coefficients') describing the deviation from the Henry's law constants in concentrated ionic solutions are available for very few species [e.g., DeBruyn *et al.*, 1995]. Currently such data sets are still too incomplete to allow a consistent use in multiphase models.

[13] Since the main focus in the present study is the development and application of the chemical mechanism, the water uptake of the organic mass formed in the cloud is simplified: The masses of moderately soluble acids (glyoxylic, oxalic, succinic and adipic acid) are split into a dissolved mass fraction and undissolved material depending on their solubility in water ( $102 \text{ g l}^{-1}$ ,  $102 \text{ g l}^{-1}$ ,  $88 \text{ g l}^{-1}$  and  $25 \text{ g l}^{-1}$ , respectively). At each time step the actual concentration of each of these acids is considered. If it exceeds the respective solubility limit, the saturation concentration is treated as dissolved mass and the excess as undissolved, i.e., insoluble mass. More soluble organic acids (formic, acetic, glycolic, malonic, glutaric and pyruvic acid) are assumed to be completely soluble since they have comparable or even greater solubilities than ammonium sulphate [Saxena and Hildemann, 1996; Lide, 2000]. The water uptake of total dissolved organic material is assumed to be identical to that of the inorganic ionic material present. It has been shown by several experimental studies that this hypothesis might be a good approximation for the dicarboxylic acids considered in the present study [e.g., Cruz and Pandis, 1998]. At each time step the ammonium, sulphate and dissolved organic masses are calculated. The water uptake of the dissolved organic mass is treated in the same manner as the existing ammonium/sulphate mixture in the aerosol present. This simplified treatment of the mixed aerosol particles might cause a biased representation of the efficiency of organic acids as cloud condensation nuclei (CCN), as most of them are less hygroscopic than ammonium sulphate but might efficiently suppress the surface tension [Facchini *et al.*, 1999]. However, laboratory studies have shown that the influence of organic acids on CCN activity is only likely to be significant if their mass fraction exceeds about 50% of the total aerosol mass [Corrigan, 2001]. A more sophisticated description of the hygroscopic properties and CCN activity of internal mixtures of organics and inorganics will be discussed in a forthcoming paper [Ervens *et al.*, 2004].

### 3. Chemical Mechanism

#### 3.1. Gas Phase Processes

[14] The model runs are performed for 12 hours starting at 6 am. Photolysis rates (reactions 55g–69g, Table 1) are

calculated for  $40^\circ\text{N}$  on June 21st at a height of 1 km. The maximum values (at local noon) for this latitude are given in Table 1. The parameterization of these rates is based on the Tropospheric and Ultraviolet radiation model (<http://www.acd.ucar.edu/TUV>) by Madronich [1993]. The photolysis rates are time dependent but not influenced by the presence of clouds. This assumption implies that the rates might be overestimated by up to a factor of 2 in and under the cloud and underestimated by the same factor at the top of the cloud [Madronich, 1987; Volz-Thomas *et al.*, 1996; Shetter *et al.*, 2002].

[15] The chemical mechanism includes reactions of ozone, OH and peroxy radicals as oxidants. Other oxidants of organics such as  $\text{NO}_3$  are not explicitly considered since the simulations are performed for daytime conditions. Most rate constants for the chemical processes in the gas phase are taken from the model used by Frost *et al.* [1998]. A constant deposition rate of  $10^{-5} \text{ s}^{-1}$  for hydrogen peroxide is applied, enabling the continuous removal of this species and controlling the  $\text{HO}_x$  budget in both the gas and aqueous phases.

[16] The organic chemistry is restricted to the oxidation of four gas phase precursors (toluene, ethylene, isoprene and cyclohexene) which are representative of different classes of anthropogenic and/or biogenic emissions. Their oxidation processes lead to oxygenated species with a higher solubility and lower vapor pressures than the precursors. The oxidation steps in the gas phase of toluene, ethylene, and isoprene are shown in Figures 1–3 and are explained in further detail in the following sections.

[17] It is likely that additional carbon containing products are formed which are not considered in the chemical mechanism. We focus only on species which might act possibly as direct precursors for dicarboxylic acids in the aqueous phase. Since we neglect additional organic species the carbon balance is not achieved in some reactions in Table 1. Thus the mechanism represents a simplification of the oxidation of the chosen organic precursors. These omissions probably lead to an overestimate of the dicarboxylic acid mass production efficiency in clouds since (1) the presence of additional organic species affects the  $\text{HO}_x$  cycle and (2) the adsorption of organic species onto the particle phase could influence the particles' hygroscopicity due to surface modification. Adsorption processes onto particles surfaces might represent efficient sinks for low volatility, hydrophobic species. It is likely that such species form a separate organic condensed phase which is not miscible with water and thus where other chemical processes occur than in the aqueous phase. Such species will contribute to the total organic aerosol mass but it is unlikely that their further chemical reactions will lead to dicarboxylic acids.

[18] Thus this reaction scheme represents a somewhat limited view of the highly complex organic chemistry. However, it does allow implementation into a coupled chemistry/microphysics model and an estimate of an upper bound of the impact of organic cloud chemistry on aerosol composition.

##### 3.1.1. Toluene

[19] Aromatic compounds represent a major contribution of anthropogenic emissions. Among these, toluene is one of the most abundant species with average concentrations of 2–39 ppb in urban, 0.05–0.8 ppb in rural and 0.01–0.25 ppb in remote areas [Finlayson-Pitts and Pitts, 2000].

**Table 1.** Gas Phase Processes<sup>a</sup>

	NO <sub>x</sub> , O <sub>3</sub> , HO <sub>x</sub> Chemistry	A or k, cm <sup>3</sup> s <sup>-1</sup>	E/R, K	Reference <sup>b</sup>
1g	NO <sub>2</sub> + O <sub>3</sub> → NO <sub>3</sub> + O <sub>2</sub>	1.2 · 10 <sup>-13</sup>	2450	1
2g	NO <sub>2</sub> + NO <sub>3</sub> → N <sub>2</sub> O <sub>5</sub>	A = 2.2 · 10 <sup>-30</sup> · (300/T) <sup>3.9</sup> · [M]; B = A/(1.5 · 10 <sup>-12</sup> · (300/T) <sup>0.7</sup> ); C = 1/(1 + (log <sub>10</sub> (B) · log <sub>10</sub> (B))) k = A/(1 + B) · 0.6 <sup>C</sup>		1
3g	N <sub>2</sub> O <sub>5</sub> → NO <sub>2</sub> + NO <sub>3</sub>	k = k <sub>2g</sub> /(2.7 · 10 <sup>-27</sup> · exp(-11000/T))		1
4g	O( <sup>1</sup> D) + H <sub>2</sub> O → 2 OH	2.2 · 10 <sup>-10</sup>		1
5g	HO <sub>2</sub> + HO <sub>2</sub> → H <sub>2</sub> O <sub>2</sub> + O <sub>2</sub>	k = 1.77 · 10 <sup>-33</sup> · [M] · exp(1000/T) + 2.3 · 10 <sup>-13</sup> · exp(600/T) · (1 + 1.4 · 10 <sup>-21</sup> · [H <sub>2</sub> O]) · exp(2200/T)		1
6g	OH + O <sub>3</sub> → HO <sub>2</sub> + O <sub>2</sub>	1.6 · 10 <sup>-12</sup>	940	1
7g	HO <sub>2</sub> + O <sub>3</sub> → OH + 2 O <sub>2</sub>	1.1 · 10 <sup>-14</sup>	500	1
8g	OH + CH <sub>4</sub> (+O <sub>2</sub> ) → CH <sub>3</sub> O <sub>2</sub> + H <sub>2</sub> O	2.45 · 10 <sup>-12</sup>	1775	1
9g	CH <sub>3</sub> O <sub>2</sub> + NO → HCHO + HO <sub>2</sub> + NO <sub>2</sub>	3 · 10 <sup>-12</sup>	-280	1
10g	HO <sub>2</sub> + NO → OH + NO <sub>2</sub>	3.5 · 10 <sup>-12</sup>	-250	1
11g	CH <sub>3</sub> O <sub>2</sub> + HO <sub>2</sub> → CH <sub>2</sub> OOH + O <sub>2</sub>	3.8 · 10 <sup>-13</sup>	-800	1
12g	OH + CO (+O <sub>2</sub> ) → CO <sub>2</sub> + HO <sub>2</sub>	k = 1.5 · 10 <sup>-13</sup> · (1 + 0.6 · [M] · 1.363 · 10 <sup>-22</sup> · T)		1
13g	NO + O <sub>3</sub> → NO <sub>2</sub> + O <sub>2</sub>	2 · 10 <sup>-12</sup>	1400	1
14g	OH + NO <sub>2</sub> → HNO <sub>3</sub>	A = 2.5 · 10 <sup>-30</sup> · (300/T) <sup>4.4</sup> · [M] B = A/(1.6 · 10 <sup>-11</sup> · (300/T) <sup>1.7</sup> ) C = 1/(1 + (log <sub>10</sub> (B) · log <sub>10</sub> (B))) k = A/(1 + B) · 0.6 <sup>C</sup>		1
15g	HO <sub>2</sub> + NO <sub>2</sub> → HNO <sub>4</sub>	A = 1.8 · 10 <sup>-31</sup> · (300/T) <sup>3.2</sup> · [M] B = A/(4.7 · 10 <sup>-12</sup> · (300/T) <sup>1.4</sup> ) C = 1/(1 + (log <sub>10</sub> (B) · log <sub>10</sub> (B))) k = A/(1 + B) · 0.6 <sup>C</sup>		1
16g	HNO <sub>4</sub> → HO <sub>2</sub> + NO <sub>2</sub>	k = k <sub>15g</sub> /(2.1 · 10 <sup>-27</sup> · exp(10900/T))		1
17g	OH + HCHO → HO <sub>2</sub> + CO + H <sub>2</sub> O	1 · 10 <sup>-11</sup>		1
18g	OH + CH <sub>3</sub> OOH → 0.67 · (CH <sub>3</sub> O <sub>2</sub> + H <sub>2</sub> O) + 0.33 · (HCHO + OH)	3.8 · 10 <sup>-11</sup>	-200	1
19g	OH + H <sub>2</sub> O <sub>2</sub> → HO <sub>2</sub> + H <sub>2</sub> O	2.9 · 10 <sup>-12</sup>	160	1
20g	OH + HO <sub>2</sub> → H <sub>2</sub> O + O <sub>2</sub>	4.8 · 10 <sup>-11</sup>	-250	1
21g	H <sub>2</sub> O <sub>2</sub> → ...	1 · 10 <sup>-5</sup>		'deposition'
22g	HNO <sub>3</sub> → ...	1 · 10 <sup>-4</sup>		'deposition'
23g	N <sub>2</sub> O <sub>5</sub> → HNO <sub>3</sub>	k [s <sup>-1</sup> ] = -35 · T <sup>0.5</sup> · surface		1
<i>Organic Chemistry: Toluene (and Its Oxidation Products)</i>				
24g	OH + CH <sub>3</sub> C <sub>6</sub> H <sub>5</sub> → HOCH <sub>2</sub> C <sub>6</sub> H <sub>5</sub> O <sub>2</sub> + H <sub>2</sub> O	1.81 · 10 <sup>-12</sup>	-355	Atkinson et al. [1997]
25g	HOCH <sub>2</sub> C <sub>6</sub> H <sub>5</sub> O <sub>2</sub> + NO → 0.67 (CHO) <sub>2</sub> + 0.65 CH <sub>3</sub> C(O)CHO + NO <sub>2</sub> + HO <sub>2</sub>	4 · 10 <sup>-12</sup>		Stockwell et al. [1997]
26g	OH + (CHO) <sub>2</sub> → HO <sub>2</sub> + CO + H <sub>2</sub> O	1.14 · 10 <sup>-11</sup>		1
27g	OH + CH <sub>3</sub> C(O)CHO → HO <sub>2</sub> + CH <sub>3</sub> C(O)O <sub>2</sub> + CO	1.72 · 10 <sup>-11</sup>		1
28g	CH <sub>3</sub> C(O)O <sub>2</sub> + NO → CH <sub>3</sub> O <sub>2</sub> + NO <sub>2</sub>	2 · 10 <sup>-11</sup>		Atkinson et al. [1997]
29g	CH <sub>3</sub> C(O)O <sub>2</sub> + HO <sub>2</sub> → CH <sub>3</sub> COOH + O <sub>3</sub>	k = 1.15 · 10 <sup>-12</sup> · exp(500/T) + 3.86 · 10 <sup>16</sup> · exp(2640/T)		Moortgat et al. [1989]
<i>Ethylene (and Its Oxidation Products)</i>				
30g	OH + C <sub>2</sub> H <sub>4</sub> → HOC <sub>2</sub> H <sub>4</sub> O <sub>2</sub> + H <sub>2</sub> O	A = 1 · 10 <sup>-28</sup> · (300/T) <sup>8.8</sup> · [M] B = A/8.8 · 10 <sup>-12</sup> C = 1/(1 + (log <sub>10</sub> (B) · log <sub>10</sub> (B))) k = A/(1 + B) · 0.6 <sup>C</sup>		1
31g	OH + HOCH <sub>2</sub> CHO → HOCH <sub>2</sub> C(O)O <sub>2</sub>	1.1 · 10 <sup>-11</sup>		Bacher et al. [2001]
32g	HOCH <sub>2</sub> C(O)O <sub>2</sub> + NO → HCHO + HO <sub>2</sub> + CO <sub>2</sub> + NO <sub>2</sub>	2 · 10 <sup>-11</sup>		estimated (k <sub>32g</sub> = k <sub>28g</sub> )
33g	HOC <sub>2</sub> H <sub>4</sub> O <sub>2</sub> + NO → 0.2 HOCH <sub>2</sub> CHO + HO <sub>2</sub> + NO <sub>2</sub> + 1.6 HCHO	9 · 10 <sup>-12</sup>		Atkinson et al. [1997]
34g	2 CH <sub>3</sub> C(O)O <sub>2</sub> → 2 CH <sub>3</sub> O <sub>2</sub> + 2 O <sub>2</sub>	2.8 · 10 <sup>-12</sup>	-530	Lightfoot et al. [1992]
35g	OH + HCOCOOH → CO <sub>2</sub> + CO + HO <sub>2</sub>	1 · 10 <sup>-13</sup>		estimated
36g	OH + HCOOH → CO <sub>2</sub> + HO <sub>2</sub> + H <sub>2</sub> O	4.5 · 10 <sup>-13</sup>		Atkinson et al. [1997]
37g	OH + CH <sub>3</sub> COOH → CH <sub>3</sub> C(O)O <sub>2</sub> + HO <sub>2</sub>	8 · 10 <sup>-13</sup>		Atkinson et al. [1997]
38g	OH + CH <sub>3</sub> OH → HCHO + HO <sub>2</sub>	6.7 · 10 <sup>-12</sup>	600	1
39g	HOCH <sub>2</sub> C(O)O <sub>2</sub> + NO → NO <sub>2</sub> + HCHO + CO <sub>2</sub>	2 · 10 <sup>-11</sup>		estimated (k <sub>39g</sub> = k <sub>28g</sub> )
40g	OH + CH <sub>3</sub> C(O)COOH → HO <sub>2</sub> + CO <sub>2</sub> + H <sub>3</sub> C(O)O <sub>2</sub>	1 · 10 <sup>-13</sup>		estimated
<i>Cyclohexene</i>				
41g	O <sub>3</sub> + C <sub>6</sub> H <sub>10</sub> → 0.3 C <sub>5</sub> difunct. + 0.05 C <sub>6</sub> difunct.	2.88 · 10 <sup>-15</sup>	1063	Finlayson-Pitts and Pitts [2000]
42g	OH + C <sub>6</sub> H <sub>10</sub> → 0.3 C <sub>6</sub> difunct.	6.73 · 10 <sup>-11</sup>		Atkinson [1986]
43g	OH + C <sub>5</sub> difunct → products	1 · 10 <sup>-12</sup>		estimated
44g	OH + C <sub>6</sub> difunct → products	1 · 10 <sup>-12</sup>		estimated

Table 1. (continued)

NO <sub>x</sub> , O <sub>3</sub> , HO <sub>x</sub> Chemistry		A or k, cm <sup>3</sup> s <sup>-1</sup>	E/R, K	Reference <sup>b</sup>
<i>Isoprene (and Its Oxidation Products)</i>				
45g	OH + C <sub>5</sub> H <sub>8</sub> → HOC <sub>5</sub> H <sub>8</sub> O <sub>2</sub>	2.54 · 10 <sup>-11</sup>	-408	<i>Finlayson-Pitts and Pitts [2000]</i> estimated (k <sub>46g</sub> = k <sub>51g</sub> )
46g	HOC <sub>5</sub> H <sub>8</sub> O <sub>2</sub> + NO → 0.45 MVK + 0.45 MACR + 0.9 NO <sub>2</sub> + 0.9 HO <sub>2</sub> + 0.9 HCHO	4.9 · 10 <sup>-12</sup>	-180	
47g	O <sub>3</sub> + C <sub>5</sub> H <sub>8</sub> → 0.05 HO <sub>2</sub> + 0.5 HCHO + 0.2 MVKp + 0.3 MACRp + 0.2 MVK + 0.2 CH <sub>2</sub> O <sub>2</sub> + 0.2 CO	7.86 · 10 <sup>-15</sup>	1919	1
48g	OH + MACR → MACRp	1.86 · 10 <sup>-11</sup>	-175	
49g	O <sub>3</sub> + MACR → 0.21 HO <sub>2</sub> + 0.15 CH <sub>3</sub> O <sub>2</sub> + 0.5 HCHO + 0.2 CH <sub>2</sub> O <sub>2</sub> + 0.7 CH <sub>3</sub> C(O)CHO	1.36 · 10 <sup>-15</sup>	2112	1
50g	OH + MVK → MVKp	4.13 · 10 <sup>-12</sup>	-452	1
51g	MVKp + NO → 0.9 NO <sub>2</sub> + 0.315 HO <sub>2</sub> + 0.585 CH <sub>3</sub> C(O)O <sub>2</sub> + 0.585 CH <sub>3</sub> C(O)OH	4.9 · 10 <sup>-12</sup>	-180	1
52g	MACRp + NO → 0.95 NO <sub>2</sub> + 0.95 HO <sub>2</sub> + 0.45 HCHO + 0.95 CH <sub>3</sub> C(O)CHO	4.9 · 10 <sup>-12</sup>	-180	1
53g	CH <sub>2</sub> O <sub>2</sub> + NO → HCHO + NO <sub>2</sub>	4.9 · 10 <sup>-12</sup>	-180	1
54g	MVK + O <sub>3</sub> → 0.2 HO <sub>2</sub> + 0.5 HCHO + 0.15 CH <sub>3</sub> CHO + 0.15 CH <sub>3</sub> C(O)O <sub>2</sub> + 0.2 CH <sub>2</sub> O <sub>2</sub> + 0.5 CH <sub>3</sub> C(O)CHO	7.51 · 10 <sup>-16</sup>	1521	1
Photolysis Processes		j <sub>max</sub> , s <sup>-1</sup>	Reference <sup>b</sup>	
55g	O <sub>3</sub> → O + O <sub>2</sub>	4.823 · 10 <sup>-5</sup>	2	
56g	NO <sub>2</sub> (+O <sub>2</sub> ) → NO + O <sub>3</sub>	1.027 · 10 <sup>-2</sup>	2	
57g	HNO <sub>3</sub> → NO <sub>2</sub> + OH	8.709 · 10 <sup>-7</sup>	2	
58g	NO <sub>3</sub> (+O <sub>2</sub> ) → NO <sub>2</sub> + O <sub>3</sub>	0.224	2	
59g	HCHO →	6.152 · 10 <sup>-5</sup>	2	
60g	HCHO → 2 HO <sub>2</sub>	4.244 · 10 <sup>-5</sup>	2	
61g	CH <sub>3</sub> OOH → HO <sub>2</sub> + OH + HCHO	7.063 · 10 <sup>-6</sup>	2	
62g	H <sub>2</sub> O <sub>2</sub> → 2 OH	1.011 · 10 <sup>-5</sup>	2	
63g	(CHO) <sub>2</sub> → 0.13 HCHO + 1.55 CO + 0.15 H <sub>2</sub>	8.699 · 10 <sup>-5</sup>	2	
64g	CH <sub>3</sub> C(O)CHO → CH <sub>3</sub> C(O)O <sub>2</sub> + CO + HO <sub>2</sub>	1.286 · 10 <sup>-4</sup>	2	
65g	CH <sub>3</sub> CHO → CH <sub>3</sub> O <sub>2</sub> + HO <sub>2</sub> + CO	8.343 · 10 <sup>-6</sup>	2	
66g	HOCH <sub>2</sub> CHO → 2 HO <sub>2</sub> + HCHO	8.343 · 10 <sup>-6</sup>	j <sub>66g</sub> = j <sub>65g</sub>	
67g	CH <sub>3</sub> C(O)CH <sub>3</sub> → CH <sub>3</sub> C(O)O <sub>2</sub>	8.703 · 10 <sup>-7</sup>	2	
68g	MACR → products	6.558 · 10 <sup>-6</sup>	2	
69g	MVK → products	5.216 · 10 <sup>-6</sup>	2	

<sup>a</sup>MVK, methylvinylketone; MACR, methacrolein; MVKp and MACRp, peroxy radicals of MVK and MACR, respectively. C<sub>5</sub> difunct and C<sub>6</sub> difunct are difunctional C<sub>5</sub> and C<sub>6</sub> compounds (see text).

<sup>b</sup>References: 1, rate constants same as used by *Frost et al.* [1998]; 2, *Madronich* [1993] (available at <http://www.acd.ucar.edu/TUV>).

It is oxidized by OH, forming an aromatic peroxy radical. The initial formation of the OH adduct is not explicitly included, as it is assumed that the subsequent reaction with oxygen is sufficiently fast leading to oxygenated ring cleavage products (Figure 1). Several studies have shown that methylglyoxal and glyoxal are formed with average yields of 65 and 67%, respectively. These products account for about 50% of the total carbon. The fate of these species is either further oxidation by the OH radical or the decay by photolysis. It can be expected that due to their high effective Henry's law constants (i.e., including hydration of the aldehydes), a significant fraction of both glyoxal and methylglyoxal will be dissolved in cloud water. Additional oxidation products include ring retaining products (e.g., benzaldehyde, benzoic acids) which can also partition into the aerosol surface, thus contributing to secondary organic aerosol mass [*Odum et al.*, 1996; *Forstner et al.*, 1997]. However, these adsorption processes and the further fate of these species within the aerosol phase are not included in the chemical mechanism since there is no evidence that their oxidation products contribute to the dicarboxylic acid mass in aerosols.

### 3.1.2. Ethylene

[20] Ethylene was chosen as one of the main proxies for anthropogenic alkenes. Its main loss process (Figure 2) is the oxidation by the OH radical, leading eventually to 20% hydroxyacetaldehyde (glycolaldehyde) and 80% formalde-

hyde [*Niki et al.*, 1981]. Hydroxyacetaldehyde can either be photolyzed (due to the lack of other data the same photolysis rate as for acetaldehyde is assumed) or react with OH. The branching ratio of the oxidation of hydroxyacetaldehyde by the OH radical yields about 20% glyoxal [*Bacher et al.*, 2001] and 80% hydroxy acetyl peroxy radical (HOCH<sub>2</sub>C(O)O<sub>2</sub>) which is further decomposed to formaldehyde and CO<sub>2</sub>. The rate constant for the latter process is assumed to be the same as that for the analogous reactions of the acetyl peroxy radical. In addition to these processes, hydroxyacetaldehyde will be efficiently dissolved in the aqueous phase (effective Henry's law constant, i.e., including hydration, K<sub>H</sub><sup>eff</sup> at 298 K = 4.1 · 10<sup>4</sup> M atm<sup>-1</sup> [*Betterton and Hoffmann*, 1988]).

### 3.1.3. Cyclohexene

[21] Cyclohexene represents a model compound for symmetrical alkenes similar to monoterpenes emitted by biogenic sources [*Aschmann et al.*, 2003]. In experimental studies by *Hatakeyama et al.* [1985] and *Kalberer et al.* [2000], it has been shown that the main products of the oxidation of cyclohexene by ozone are C<sub>5</sub> and C<sub>6</sub> difunctional compounds (diols, dialdehydes, dicarboxylic acids or mixed functional groups) with average overall yields of about 30% and about 5%, respectively. The most abundant product observed in the reaction of cyclohexene with OH is pentanal and some other smaller carbonyl compounds.

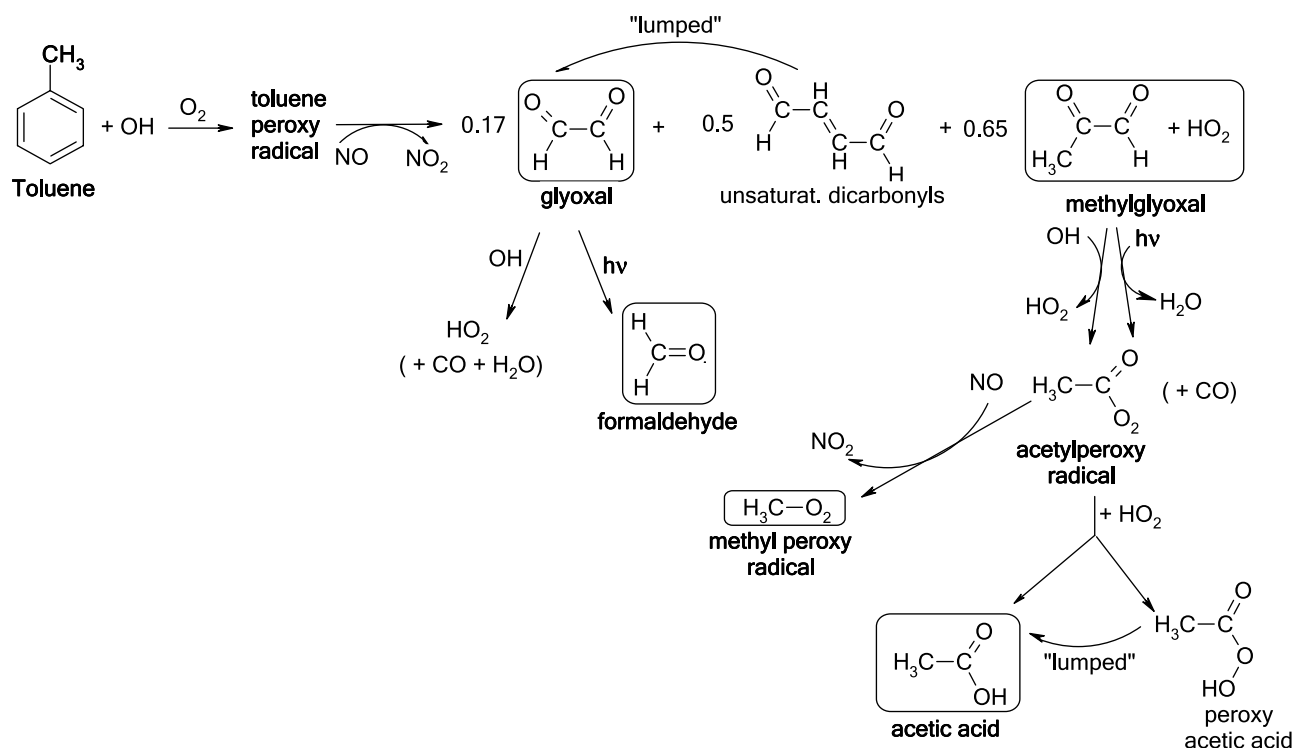


**Figure 1.** Oxidation of toluene by OH in the gas phase; in boxes: direct organic precursors are taken up by the aqueous phase.

However, the solubility of pentanal is too low ( $K_H = 6.4 \text{ M atm}^{-1}$  [Sander, 1999]) to allow an efficient dissolution into the aqueous phase. The main difunctional compound reported by Grosjean *et al.* [1996] is adipaldehyde. We assumed here a yield of 30% for this species which might represent an upper limit for the yield of difunctional compounds. We have not considered any other products even though the carbon balance for this reaction is not achieved. This is because we neglect any further products which do not contribute to the formation processes of the dicarboxylic acids in the aqueous phase.

[22] It is assumed that the fraction of all difunctional C<sub>5</sub> and C<sub>6</sub> compounds taken up by the aqueous phase will be converted completely to glutaric and adipic acid which gives an upper bound for the contribution of these processes to the dicarboxylic acid mass. In addition, gas phase sinks by OH for these compounds (R-43 g and R-44 g, Table 1) are considered with rate constants of  $10^{-12} \text{ cm}^3 \text{ s}^{-1}$  (comparable to OH reactions of noncyclic C<sub>5</sub> and C<sub>6</sub> dicarbonyl compounds). Their oxidation in the gas phase will lead to products with shortened carbon chains (<C<sub>5</sub>), but possible products are not further specified here.

### 3.1.4. Isoprene

[23] Isoprene is the major organic compound emitted by plants with emission rates far exceeding those of other biogenic species. Comparable concentrations of isoprene have been found in both urban and remote continental environments [Chameides *et al.*, 1992; Goldan *et al.*, 1995, 2000]. Based on observations it has been assumed that in a rural atmosphere pyruvic acid, the direct oxidation product of methylglyoxal found in particles, originates

mainly from direct or secondary biogenic sources, such as isoprene [Talbot *et al.*, 1995].

[24] Attack of isoprene by ozone and the OH radical both lead to the oxidation products methyl vinyl ketone (MVK) and methacrolein (MACR), with different yields for the two reaction channels (Figure 3 and Table 1). Both of these compounds are also oxidized by ozone and OH, leading to shorter carbon chain products such as formaldehyde, methyl peroxy radicals, and methylglyoxal. The products of the photolysis processes of MACR and MVK are not specified in the present mechanism. It has been shown that the rates of such photolysis processes are negligible compared to the competing OH reaction [e.g., Gierczak *et al.*, 1997], so that the subsequent products of the photolysis can be neglected.

[25] The oxidation scheme (Figure 3) shows only two major products that can act as precursors for dicarboxylic acids, methylglyoxal and hydroxyacetaldehyde. Contributions of additional products (e.g., organic nitrates) are not included although they might have a sufficiently low vapor pressure to contribute to the organic aerosol mass. Since the Henry's law constants of both methacrolein and methyl vinyl ketone are small ( $K_H(\text{MACR}) = 6.5 \text{ M atm}^{-1}$ ;  $K_H(\text{MVK}) = 41 \text{ M atm}^{-1}$  [Iraci *et al.*, 1998]), and because their aqueous phase oxidation products have not been analyzed in laboratory studies, their uptake and chemical processes in the aqueous phase are neglected.

[26] This simplified isoprene oxidation gas phase mechanism was taken from the model used by Frost *et al.* [1998]. The actual product distribution from oxidation of isoprene by OH or ozone is probably much more complex [Grosjean *et al.*, 1993; Pöschl *et al.*, 2000]. However, for the purpose of the current study, the mechanism reflects the ability

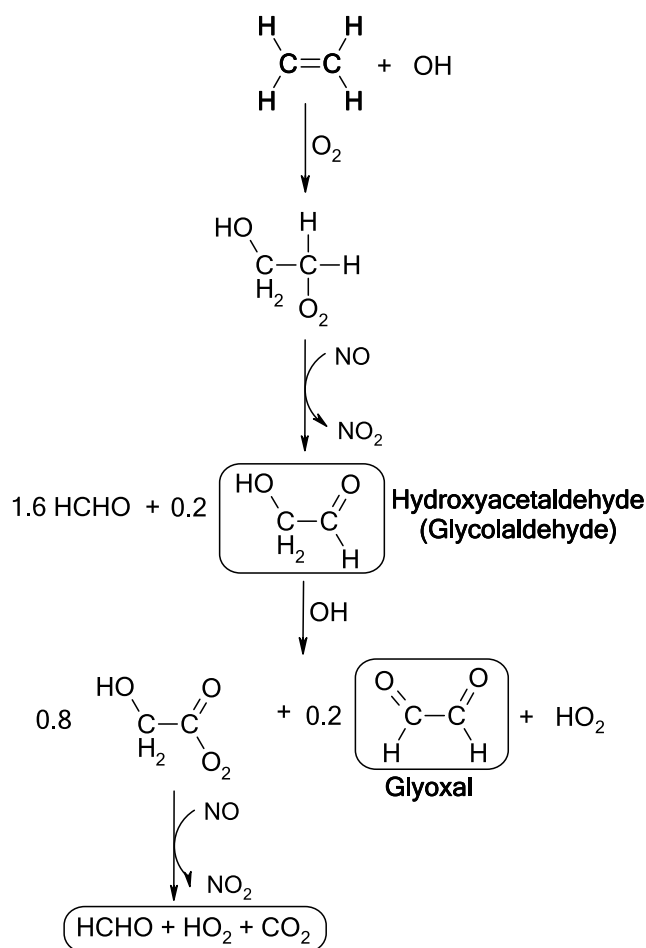


**Figure 2.** Oxidation of ethylene by OH in the gas phase; in boxes: direct organic precursors are taken up by the aqueous phase.

of isoprene to act as an indirect precursor for soluble organic compounds, in particular methylglyoxal and hydroxyacetaldehyde.

### 3.2. Aqueous Phase Processes

[27] While many gas phase oxidation schemes for organic species exist, databases for aqueous phase processes are much more limited. The chemical processes and corresponding data for the description of sulphur, organic ( $\leq \text{C}_2$ ) and  $\text{HO}_x$  aqueous chemistry are taken mainly from CAPRAM2.4 [Ervens *et al.*, 2003a]. Photolysis processes in the aqueous phase are not considered. Besides the incomplete description of the  $\text{HO}_x$  cycle, this omission might lead to an overestimate of the oxalate concentration because it is efficiently photo-oxidized if it is complexed by iron. There are few data available for the photolysis processes of carbonyl compounds in the aqueous phase. Based on a study by Faust *et al.* [1997] it can be estimated that these processes do not represent a significant loss for these species in the aqueous phase since their photolysis rates ( $j_{\text{max}} \approx 2 \cdot 10^{-4} \text{ s}^{-1}$ ) are too small to compete with the simultaneous OH reactions.

[28] All oxidation processes of organic compounds are described by reactions with the OH radical because it has been shown that the contributions of other radicals and

radical anions are negligible [Ervens *et al.*, 2003a]. For the sake of simplification and because of a lack of other mechanistic evidence, it is assumed that the oxidation of organics always occurs via H-atom abstraction by the OH radical. Unknown rate constants are estimated based on correlations between the C-H bond strength and the rate constant for the OH reaction [Ervens *et al.*, 2003b]. Recombination of the peroxy radicals (or reaction with the more abundant  $\text{HO}_2$  radical) leads to the corresponding keto and hydroxy acid (Figure 4). Unlike the analogous peroxy radical conversion in the gas phase, the reaction with NO does not occur in the aqueous phase due to the low Henry's law constant of NO ( $K_{\text{H}}(\text{NO}) \approx 10^{-3} \text{ M atm}^{-1}$  [Sander, 1999]). A schematic overview of the aqueous phase reactions is given in Figure 5; the corresponding rate constants are summarized in Table 2.

[29] While in the gas phase the oxidation of carbonyl compounds usually leads to the shortening of the carbon chain, in the aqueous phase the products are different due to stabilizing effects of the hydration shell and, in the case of aldehydes, hydration. For instance, OH oxidation or photolysis of glyoxal in the gas phase leads to  $\text{HO}_2$  and CO or  $\text{HO}_2$ , CO and formaldehyde, respectively. In the aqueous phase photolysis does not occur because glyoxal is present as the geminal diol due to its high hydration constant ( $K_{\text{Hydr}} = 3 \cdot 10^5 \text{ M}^{-1}$  [Betterson and Hoffmann, 1988]). Product studies of the OH reaction in the aqueous phase have shown that glyoxylic acid represents an oxidation product of glyoxal and might be further oxidized to oxalic acid [Karpel vel Leitner and Doré, 1997].

[30] As suggested in 3.1.3 glutaric and adipic acid represent the products from gas phase oxidation of cyclohexene by ozone which are taken up by the aqueous phase. Based on the suggestion by Kawamura and Sakaguchi [1999], glutaric and adipic acid are oxidized and their decay leads to smaller dicarboxylic organic acids. The initial step is the attack of OH on the weakest C-H bond (next to the acid groups) followed by the formation of the peroxy radical (Figure 4). A rate constant of  $1 \cdot 10^7 \text{ M}^{-1} \text{ s}^{-1}$  was estimated for the overall OH reaction of adipic and glutaric acid, which is slightly smaller than those for the smaller acids, succinic and malonic acid ( $k = 5 \cdot 10^7 \text{ M}^{-1} \text{ s}^{-1}$ ). The rate coefficients for the straight (unsubstituted) dicarboxylic acids increase with increasing carbon number. However, the oxidation reactions of the dicarboxylic acids are lumped processes in the current mechanism, including the formation and further reaction of the hydroxy and keto dicarboxylic acids. The intermediate keto dicarboxylic acids resulting from the OH reactions are quite unstable due to three carbonyl groups within the relatively short carbon chain. Stabilization is achieved by decarboxylation leading to a keto monocarboxylic acid, which is further oxidized. However, no rate constants are available for these elementary reactions in the aqueous phase. It was assumed that an increasing number of carbonyl groups within the relatively small carbon chains leads to a decreasing stability and thus to a higher reactivity of the smaller substituted dicarboxylic acids.

[31] In general, these rate constants seem to be small compared to those of other OH reactions, but with this conservative estimate, possible incomplete conversion by side reactions is partially taken into account. Due to the significant lack of product studies in the aqueous phase a more detailed mechanism based on well-founded data

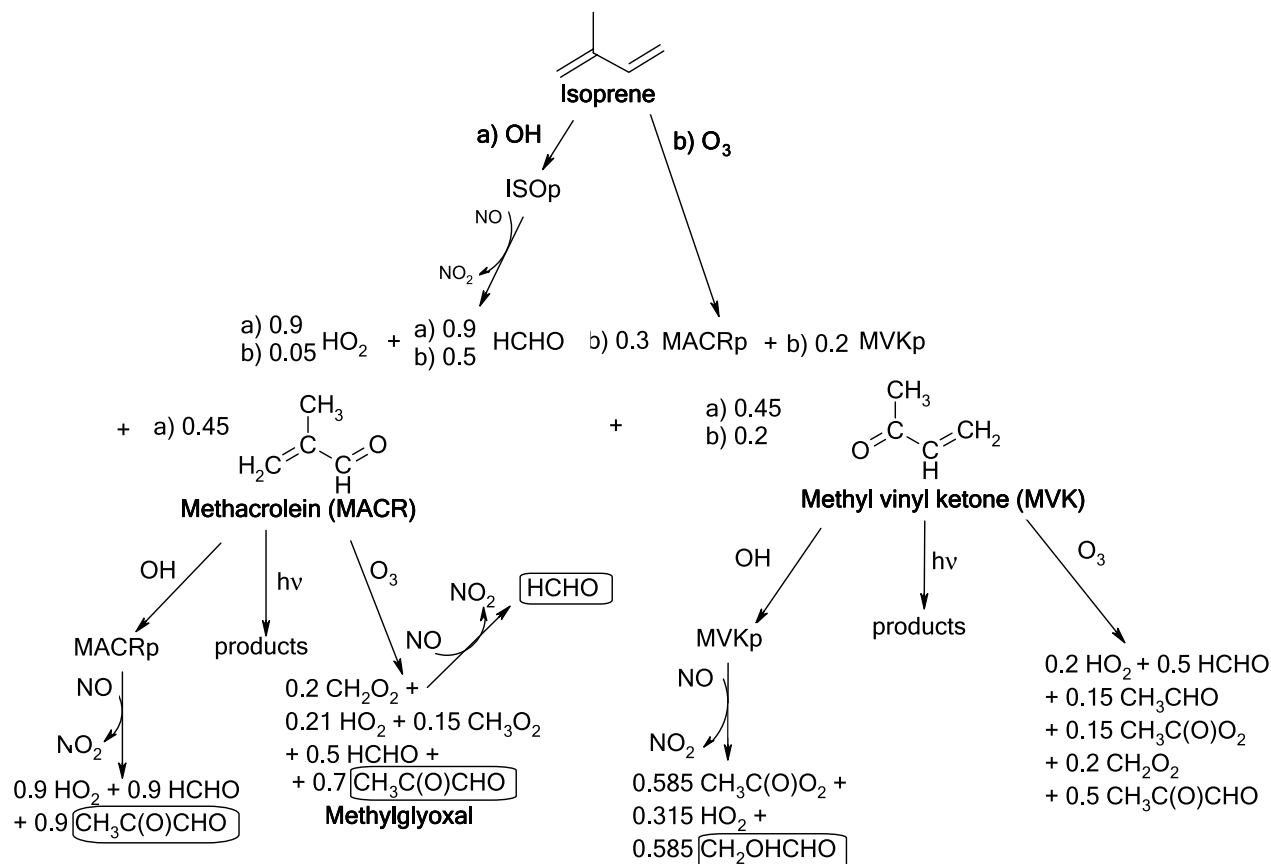


**Figure 3.** Oxidation of isoprene by (a) O<sub>3</sub> and (b) OH in the gas phase; in boxes: direct organic precursors are taken up by the aqueous phase.

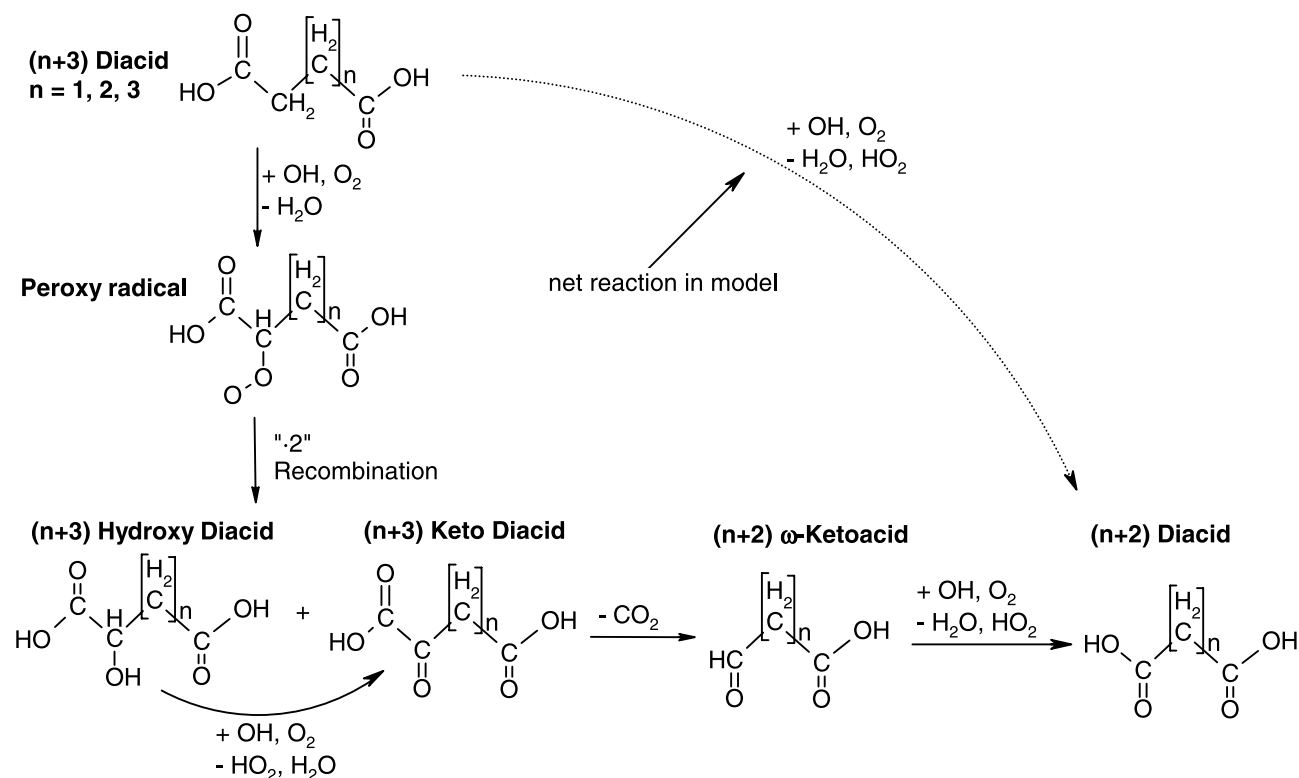


**Figure 4.** Decarboxylation mechanism of dicarboxylic acids in the aqueous phase by OH.

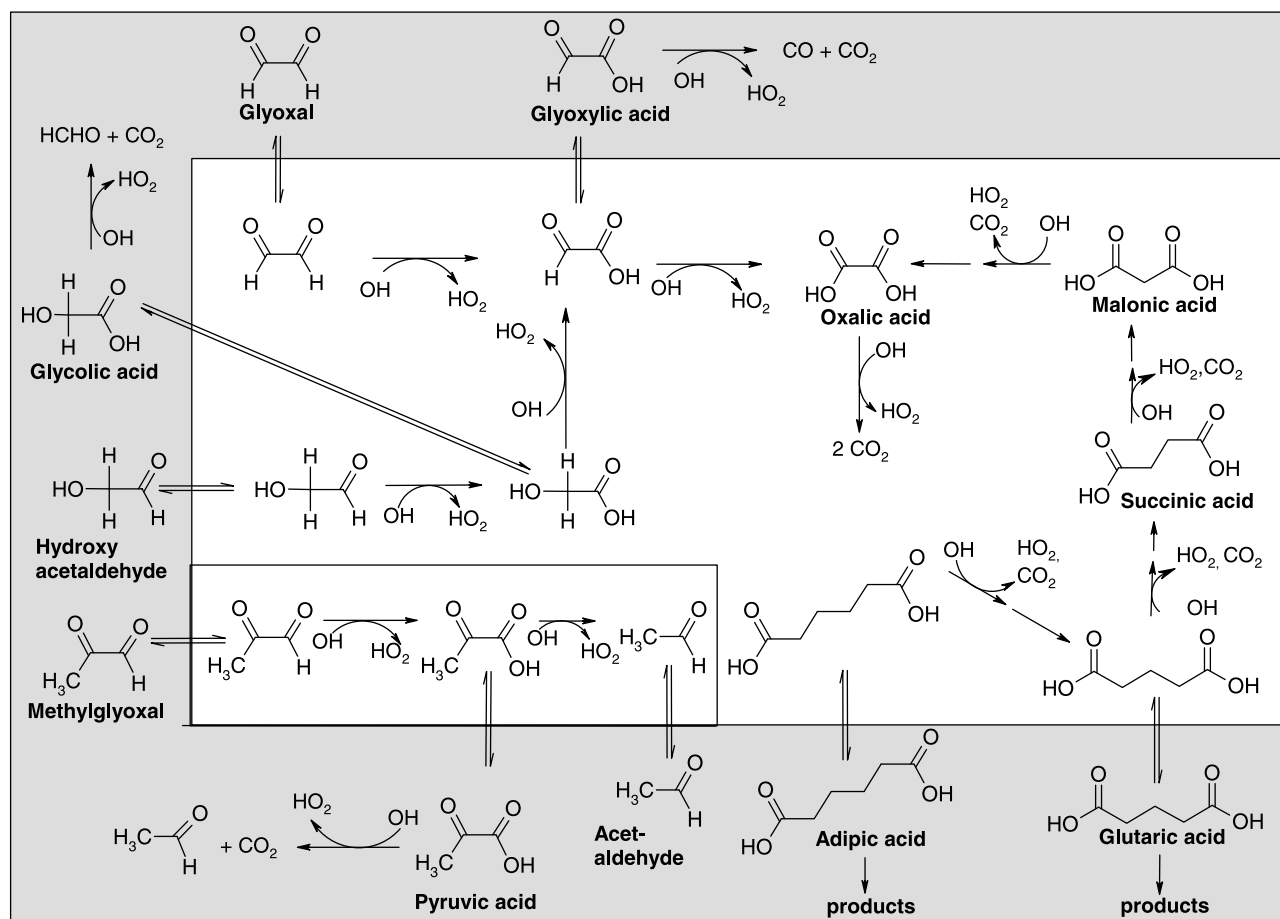


Figure 5. Multiphase organic chemistry (shaded area: gas phase).

cannot be formulated here. In addition, we neglect other more volatile products which might evaporate and thus do not contribute to the aerosol mass. Similar mechanisms might represent formation pathways of the corresponding hydroxy and/or keto derivatives (Figure 4), such as malic and tartaric acid, which have also been identified as aerosol components [e.g., Neusüß *et al.*, 2000]. These intermediate products also have finite lifetimes and thus might contribute to the organic aerosol mass. Thus the assumption of a ‘delayed’ oxidation (and thus enhanced lifetime) of the dicarboxylic acids seems appropriate.

### 3.3. Uptake Processes

[32] Exchange processes between the gas and aqueous phase are described according to the resistance model of Schwartz [1986] considering mass accommodation ( $\alpha$ ), gas phase diffusion ( $D_g$ ) and Henry’s law constants ( $K_H$ ) for each soluble species (Table 3). All data in Table 3 describe uptake processes on aqueous surfaces, i.e., on dilute particles. It has been shown that the uptake coefficients of trace gases on organic surfaces, e.g., due to adsorption of hydrophobic organics on existing particles is significantly lower than on dilute particles. Thus the restriction of uptake processes to dilute droplets might represent an overestimate of the uptake efficiency of the aqueous phase, and thus of the mass production rates within the cloud droplets.

[33] It is assumed that the vapor pressures of sulphate (sulphuric acid), oxalic acid, succinic acid and malonic acid

are sufficiently low ( $<10^{-5}$  mm Hg) so that no evaporation of these species occurs [Saxena and Hildemann, 1996]. Based on this limit for the vapor pressure, the organic species shown in Figure 5 were separated into volatile and nonvolatile species, respectively. Furthermore, hydroxymethanesulfonate does not evaporate as only its single components, i.e., formaldehyde and sulphur(IV), are volatile.

### 3.4. Initial Conditions

[34] In the current study two different scenarios are discussed to allow a differentiation between polluted and clean continental conditions. The initial concentrations of gas phase species are given in Table 4. For both cases an identical initial aerosol size distribution is assumed. However, in the polluted case the number concentration is  $N = 500 \text{ cm}^{-3}$ , and in the clean continental case  $N = 100 \text{ cm}^{-3}$ .

[35] Concentrations of highly abundant gas phase species, such as  $\text{CH}_4$  and CO are held constant for all model runs. The initial concentrations of oxygenated organic gas phase species are obtained from off-line model runs considering only gas phase chemistry without any particle phase. These runs were initialized with the indicated concentrations of reduced organic species and ‘key species,’ such as CO and  $\text{NO}_x$ . Radical species’ concentrations are initially set to zero since they are produced by photochemical processes. The model runs are performed for a closed system; i.e., there is no renewal of the

**Table 2.** Aqueous Phase Processes

	Equilibria	K, M	E/R, K	Reference <sup>a</sup>
1eq	SO <sub>2</sub> (+H <sub>2</sub> O) HSO <sub>3</sub> <sup>-</sup> + H <sup>+</sup>	1.74 · 10 <sup>-2</sup>	1940	3
2eq	HSO <sub>3</sub> <sup>-</sup> SO <sub>3</sub> <sup>2-</sup> + H <sup>+</sup>	6.22 · 10 <sup>-8</sup>	1960	3
3eq	H <sub>2</sub> SO <sub>4</sub> HSO <sub>4</sub> <sup>-</sup> + H <sup>+</sup>	1000		
4eq	HSO <sub>4</sub> <sup>-</sup> SO <sub>4</sub> <sup>2-</sup> + H <sup>+</sup>	1.02 · 10 <sup>-2</sup>	2700	3
5eq	HNO <sub>3</sub> NO <sub>3</sub> <sup>-</sup> + H <sup>+</sup>	22	1800	3
6eq	NH <sub>3</sub> (+H <sub>2</sub> O) NH <sub>4</sub> <sup>+</sup> + OH <sup>-</sup>	1.76 · 10 <sup>-5</sup>	-560	3
7eq	H <sub>2</sub> O H <sup>+</sup> + OH <sup>-</sup>	1 · 10 <sup>-14</sup>	-6710	3
8eq	CO <sub>2</sub> (+H <sub>2</sub> O) HCO <sub>3</sub> <sup>-</sup> + H <sup>+</sup>	7.7 · 10 <sup>-7</sup>	-1000	<i>Graedel and Weschler</i> [1981]
9eq	HCO <sub>3</sub> <sup>-</sup> CO <sub>3</sub> <sup>2-</sup> + H <sup>+</sup>	4.84 · 10 <sup>-11</sup>	-1760	<i>Graedel and Weschler</i> [1981]
10eq	HO <sub>2</sub> O <sub>2</sub> <sup>-</sup> + H <sup>+</sup>	1.6 · 10 <sup>-5</sup>		3
11eq	HCOCOOH HCOCOO <sup>-</sup> + H <sup>+</sup>	6.6 · 10 <sup>-4</sup>		<i>Lide</i> [2000]
12eq	HCOOH HCOO <sup>-</sup> + H <sup>+</sup>	1.77 · 10 <sup>-5</sup>		3
13eq	CH <sub>3</sub> C(O)COOH CH <sub>3</sub> C(O)COO <sup>-</sup> + H <sup>+</sup>	4.07 · 10 <sup>-3</sup>		<i>Lide</i> [2000]
14eq	CH <sub>3</sub> COOH CH <sub>3</sub> COO <sup>-</sup> + H <sup>+</sup>	1.77 · 10 <sup>-4</sup>		3
15eq	(COOH) <sub>2</sub> HC <sub>2</sub> O <sub>4</sub> <sup>-</sup> + H <sup>+</sup>	6.4 · 10 <sup>-2</sup>		3
16eq	HC <sub>2</sub> O <sub>4</sub> <sup>-</sup> C <sub>2</sub> O <sub>4</sub> <sup>2-</sup> + H <sup>+</sup>	5.25 · 10 <sup>-5</sup>		3
	Irreversible Reactions	k, M <sup>-1</sup> s <sup>-1</sup>	E/R, K	Reference <sup>a</sup>
1aq	SO <sub>2</sub> + O <sub>3</sub> → S(VI) + O <sub>2</sub>	2.4 · 10 <sup>4</sup>		3
2aq	HSO <sub>3</sub> <sup>-</sup> + O <sub>3</sub> → (VI) + O <sub>2</sub>	3.7 · 10 <sup>5</sup>	5530	3
3aq	SO <sub>3</sub> <sup>2-</sup> + O <sub>3</sub> → (VI) + O <sub>2</sub>	1.5 · 10 <sup>9</sup>	5280	3
4aq	H <sub>2</sub> O <sub>2</sub> + HSO <sub>3</sub> <sup>-</sup> + H <sup>+</sup> → S(VI) + H <sub>2</sub> O	7.2 · 10 <sup>7</sup> M <sup>-2</sup> s <sup>-1</sup>	4000	3
5aq	NO <sub>3</sub> → NO <sub>3</sub> <sup>-</sup>	1000 s <sup>-1</sup>	4300	3 <sup>b</sup>
6aq	HO <sub>2</sub> + HO <sub>2</sub> → H <sub>2</sub> O <sub>2</sub> + O <sub>2</sub>	8.3 · 10 <sup>5</sup>	2720	3
7aq	O <sub>2</sub> <sup>-</sup> + HO <sub>2</sub> (+H <sup>+</sup> ) → H <sub>2</sub> O <sub>2</sub> + O <sub>2</sub>	9.7 · 10 <sup>7</sup>	1060	3
8aq	OH + CH <sub>2</sub> (OH) <sub>2</sub> → HO <sub>2</sub> + HCOOH	1 · 10 <sup>9</sup>	1020	3
9aq	OH + CH <sub>3</sub> OOH → CH <sub>3</sub> O <sub>2</sub> + H <sub>2</sub> O	2.4 · 10 <sup>7</sup>	1680	3
10aq	OH + CH <sub>3</sub> OOH → HO <sub>2</sub> + HCOOH	6 · 10 <sup>6</sup>	1680	3
11aq	O <sub>3</sub> + O <sub>2</sub> <sup>-</sup> → OH + 2 O <sub>2</sub> + OH <sup>-</sup>	1.5 · 10 <sup>9</sup>	2200	3
12aq	OH + (CH(OH)) <sub>2</sub> → HO <sub>2</sub> + CHOCOOH	1.1 · 10 <sup>9</sup>	1516	3
13aq	OH + CHOCOOH → HO <sub>2</sub> + (COOH) <sub>2</sub>	3.6 · 10 <sup>8</sup>	1000	<i>Ervens et al.</i> [2003b]
14aq	OH + CHOCOO <sup>-</sup> → HO <sub>2</sub> + (COOH) <sub>2</sub>	2.9 · 10 <sup>9</sup>	4300	<i>Ervens et al.</i> [2003b]
15aq	OH + CH <sub>3</sub> C(O)CHO → HO <sub>2</sub> + CH <sub>3</sub> C(O)COOH	1.1 · 10 <sup>9</sup>	1600	<i>Ervens et al.</i> [2003b]
16aq	OH + CH <sub>2</sub> OHCHO → HO <sub>2</sub> + (CH(OH)) <sub>2</sub>	1.2 · 10 <sup>9</sup>		k <sub>16aq</sub> = k <sub>17aq</sub>
17aq	OH + CH <sub>2</sub> OHCOOH → HO <sub>2</sub> + CHOCOOH	1.2 · 10 <sup>9</sup>		<i>Logan</i> [1989] (anion)
18aq	OH + C <sub>2</sub> O <sub>4</sub> <sup>2-</sup> → O <sub>2</sub> <sup>-</sup> + 2 CO <sub>2</sub> + OH <sup>-</sup>	1.6 · 10 <sup>8</sup>	4300	<i>Ervens et al.</i> [2003b]
19aq	OH + HC <sub>2</sub> O <sub>4</sub> <sup>-</sup> → HO <sub>2</sub> + 2 CO <sub>2</sub> + OH <sup>-</sup>	1.9 · 10 <sup>8</sup>	2800	<i>Ervens et al.</i> [2003b]
20aq	OH + H <sub>2</sub> C <sub>2</sub> O <sub>4</sub> → HO <sub>2</sub> + 2 CO <sub>2</sub> + H <sub>2</sub> O	1.4 · 10 <sup>6</sup>		3
21aq	OH + CH <sub>3</sub> C(O)COO <sup>-</sup> → HO <sub>2</sub> + CO <sub>2</sub> + CH <sub>3</sub> COO <sub>2</sub>	7 · 10 <sup>8</sup>		<i>Ervens et al.</i> [2003b]
22aq	OH + CH <sub>3</sub> C(O)COOH → HO <sub>2</sub> + H <sub>2</sub> O + CH <sub>3</sub> CHO	1.2 · 10 <sup>8</sup>		<i>Ervens et al.</i> [2003b]
23aq	CH <sub>2</sub> (OH) <sub>2</sub> + HSO <sub>3</sub> <sup>-</sup> → HMS <sup>-</sup>	0.436	2990	3
24aq	HMS <sup>-</sup> → CH <sub>2</sub> (OH) <sub>2</sub> + HSO <sub>3</sub> <sup>-</sup>	1.22 · 10 <sup>-7</sup>		3
25aq	CH <sub>2</sub> (OH) <sub>2</sub> + SO <sub>3</sub> <sup>2-</sup> → HMS <sup>-</sup>	1.36 · 10 <sup>5</sup>	2450	3
26aq	HMS <sup>-</sup> → CH <sub>2</sub> (OH) <sub>2</sub> + SO <sub>3</sub> <sup>2-</sup>	3.8 · 10 <sup>-6</sup>	5530	3
27aq	HMS <sup>-</sup> + OH → HO <sub>2</sub> + HCOOH + HSO <sub>3</sub> <sup>-</sup>	3 · 10 <sup>8</sup>		3
28aq	OH + HCOO <sup>-</sup> → HO <sub>2</sub> + CO <sub>2</sub> + H <sub>2</sub> O	3.2 · 10 <sup>9</sup>	1000	3
29aq	OH + HCOOH → HO <sub>2</sub> + CO <sub>2</sub> + H <sub>2</sub> O	1.3 · 10 <sup>8</sup>	1000	3
30aq	OH + CH <sub>3</sub> COO <sup>-</sup> → HO <sub>2</sub> + OH <sup>-</sup> + CH <sub>3</sub> C(O)O <sub>2</sub>	1 · 10 <sup>8</sup>	1800	3
31aq	OH + CH <sub>3</sub> COOH → HO <sub>2</sub> + H <sub>2</sub> O + CH <sub>3</sub> C(O)O <sub>2</sub>	1.5 · 10 <sup>7</sup>	1330	3
32aq	CH <sub>3</sub> O <sub>2</sub> + CH <sub>3</sub> O <sub>2</sub> → HCHO + CH <sub>3</sub> OH + HO <sub>2</sub>	1.7 · 10 <sup>8</sup>	2200	3
33aq	H <sub>2</sub> O <sub>2</sub> + OH → HO <sub>2</sub> + H <sub>2</sub> O	3 · 10 <sup>7</sup>	1680	3
34aq	OH + CH <sub>3</sub> OH → HO <sub>2</sub> + CH <sub>2</sub> (OH) <sub>2</sub>	1 · 10 <sup>9</sup>	580	3
35aq	OH + C <sub>4</sub> H <sub>8</sub> (COOH) <sub>2</sub> → C <sub>3</sub> H <sub>6</sub> (COOH) <sub>2</sub> + HO <sub>2</sub>	1 · 10 <sup>7</sup>		estimated (k <sub>35aq</sub> = 0.2 · k <sub>37aq</sub> )
36aq	OH + C <sub>3</sub> H <sub>6</sub> (COOH) <sub>2</sub> → C <sub>2</sub> H <sub>4</sub> (COOH) <sub>2</sub> + HO <sub>2</sub>	1 · 10 <sup>7</sup>		estimated (k <sub>36aq</sub> = 0.2 · k <sub>37aq</sub> )
37aq	OH + C <sub>2</sub> H <sub>4</sub> (COOH) <sub>2</sub> → HO <sub>2</sub> + CH <sub>2</sub> (COOH) <sub>2</sub>	5 · 10 <sup>7</sup>		estimate for overall reaction, k <sub>average</sub> [C <sub>2</sub> H <sub>4</sub> (COOH) <sub>2</sub> /HOCC <sub>2</sub> H <sub>4</sub> COO <sup>-</sup> / C <sub>2</sub> H <sub>4</sub> (COO <sup>-</sup> ) <sub>2</sub> ] <i>Ervens et al.</i> [2003b]
38aq	OH + CH <sub>2</sub> (COOH) <sub>2</sub> → HO <sub>2</sub> + (COOH) <sub>2</sub>	5 · 10 <sup>7</sup>		estimate for overall reaction, k <sub>average</sub> [CH <sub>2</sub> (COOH) <sub>2</sub> /HOCC <sub>2</sub> H <sub>4</sub> COO <sup>-</sup> / CH <sub>2</sub> (COO <sup>-</sup> ) <sub>2</sub> ] <i>Ervens et al.</i> [2003b]

<sup>a</sup>Reference: 3, data adopted from *Ervens et al.* [2003a, and references therein].

<sup>b</sup>General first-order loss process for NO<sub>3</sub>.

initialized gas phase species (except those with constant concentrations).

[36] The choices of initial SO<sub>2</sub> and aqueous-phase oxidant (primarily H<sub>2</sub>O<sub>2</sub>, but including O<sub>3</sub>) concentrations will largely determine the magnitude of sulphate produc-

tion. We note that there is sufficient initial H<sub>2</sub>O<sub>2</sub> to completely oxidize the quite low initial SO<sub>2</sub> in the clean continental case, but even if all sulphur(IV) is oxidized, the maximum aerosol sulphate mass increase is only 10%. For the polluted case, there is sufficient initial H<sub>2</sub>O<sub>2</sub> to

**Table 3.** Uptake Processes

	Species	$K_{H,i}$ , M atm <sup>-1</sup>	$\Delta H/R$ , K	$\alpha$	$D_{g,i}$ , cm <sup>2</sup> s <sup>-1</sup>	Reference <sup>a</sup>
1upt	SO <sub>2</sub>	1.24	3247	0.035	0.128	3
2upt	H <sub>2</sub> O <sub>2</sub>	$1.02 \cdot 10^5$	6340	0.05	0.148	3
3upt	HNO <sub>3</sub>	$2.1 \cdot 10^5$	8700	0.11	0.146	3
4upt	O <sub>3</sub>	$1.14 \cdot 10^{-2}$	2300	0.04	0.23	3
5upt	NH <sub>3</sub>	60.7	3920	0.054	0.132	3
6upt	CO <sub>2</sub>	$3.1 \cdot 10^{-2}$	2423	$2 \cdot 10^{-4}$	0.155	3
7upt	NO <sub>3</sub>	0.6		$4 \cdot 10^{-3}$	0.1	3
8upt	OH	25	5280	0.1	0.11	3
9upt	HO <sub>2</sub>	9000		0.05	0.153	3
10upt	HCHO	4998 <sup>b</sup>		0.01	0.104	3
11upt	CH <sub>3</sub> O <sub>2</sub>	310		0.02	0.164	3
12upt	CH <sub>3</sub> OOH	310		$3.8 \cdot 10^{-3}$	0.135	3
13upt	(CHO) <sub>2</sub>	$3 \cdot 10^{5b}$		$3.8 \cdot 10^{-3}$	0.131	3
14upt	CH <sub>3</sub> C(O)CHO	3710		0.023	0.115	Saxena and Hildemann [1996]
15upt	CH <sub>2</sub> OHCHO	$4.14 \cdot 10^4$		0.03	0.195	Betterton and Hoffmann [1988]
16upt	C <sub>5</sub> difunct	$1 \cdot 10^8$		0.01	0.1	estimated ( $K_{H,i}$ (glutaric acid)) Saxena and Hildemann [1996]
17upt	C <sub>6</sub> difunct	$1 \cdot 10^8$		0.01	0.1	estimated ( $K_{H,i}$ (adipic acid)) Saxena and Hildemann [1996]
18upt	CH <sub>3</sub> COOH	5500	5890	0.019	0.124	3
19upt	CHOCOOH	9000		0.1	0.1	Saxena and Hildemann [1996]
20upt	CH <sub>2</sub> OHCOOH	9000		0.1	0.1	estimated ( $K_{H,20upt} = K_{H,19upt}$ )
21upt	HCOOH	5530	5630	0.1	0.1	3
22upt	CH <sub>3</sub> C(O)COOH	$3.11 \cdot 10^5$	5100	0.1	0.1	Saxena and Hildemann [1996]
23upt	CH <sub>3</sub> OH	220	5390	0.015	0.1	3

<sup>a</sup>Reference: 3, data adopted from *Ervens et al.* [2003a, and references therein].

<sup>b</sup>Effective Henry's law constants (including hydration of aldehydes).

oxidize about half of the initial S(IV), which represents a potential mass addition to the initial sulphate aerosol of a factor of 25. However, due to the oxidation of the high concentrations of organics, HO<sub>2</sub> will be formed which is a major source for H<sub>2</sub>O<sub>2</sub> in both the gas and aqueous phases.

## 4. Results and Discussion

### 4.1. Increase of Total Aerosol Mass

[37] The modification of aerosol sizes by mass addition due to aqueous phase processes can influence subsequent clouds. It has been shown that in polluted scenarios the sulphate mass can be increased by more than a few hundred percent [*Beilke and Gravenhorst*, 1978; *Hoffmann*, 1986; *Feingold and Kreidenweis*, 2002]. It is obvious that this effect will only be significant if high SO<sub>2</sub> concentrations are present. However, in the following we will present additional pathways for mass formation and consider scenarios in which they might be efficient.

[38] In Figure 6a we show concentration profiles for the most effective oxidants in the gas phase (OH and O<sub>3</sub>). Due to the initially high organic concentrations there is an increase of ozone in both scenarios within the first hours of simulation. With decreasing organic and NO<sub>x</sub> concentration levels the ozone concentration decreases after a few hours. The OH concentrations do not differ significantly in both scenarios. Figure 6b shows the concentrations of the most important oxidants (OH and H<sub>2</sub>O<sub>2</sub>) in the aqueous phase. The aqueous phase concentrations represent average concentrations for all droplets, weighted by the corresponding liquid water content in each drop size class.

[39] In Figures 7a and 7b the evolution of both the total organic and ammonium sulphate masses is shown for the two cases (polluted and clean continental) discussed here. The total initial aerosol masses (pure ammonium sulphate) are  $1.8 \mu\text{g m}^{-3}$  ('polluted,'  $N = 500 \text{ cm}^{-3}$ ) and  $0.36 \mu\text{g m}^{-3}$

('clean continental,'  $N = 100 \text{ cm}^{-3}$ ), respectively. The results shown in Figure 7 represent the total ammonium sulphate and organic masses at the end of each cloud cycle. The organic mass consists of contributions of all organic acids. The ammonium sulphate mass is the sum of ammonium and sulphate; i.e., it might also include ammonium bisulphate (NH<sub>4</sub>HSO<sub>4</sub>) and sulphuric acid (H<sub>2</sub>SO<sub>4</sub>).

[40] In the polluted case there is a significant increase in the ammonium sulphate mass during the first hour caused by the high initial SO<sub>2</sub> concentration (10 ppb), leading to a relative mass addition of about one order of magnitude

**Table 4.** Initial Concentrations<sup>a</sup>

	Polluted	Clean Continental
SO <sub>2</sub>	10	0.01
O <sub>3</sub>	100	30
H <sub>2</sub> O <sub>2</sub>	5	0.2
NH <sub>3</sub>	2	0.1
HNO <sub>3</sub>	10	0.1
CO <sub>2</sub>	360 ppm	360 ppm
N <sub>2</sub> O <sub>5</sub>	0.02	0.02
HCHO	10	1
CH <sub>2</sub> OHCHO	1	0.1
(CHO) <sub>2</sub>	1	0.01
CH <sub>3</sub> C(O)CHO	1	0.01
HCOOH	0.5	0.1
CH <sub>3</sub> COOH	1	0.1
C <sub>6</sub> H <sub>5</sub> CH <sub>3</sub> (toluene)	10	0.01
C <sub>2</sub> H <sub>4</sub> (ethylene)	20	0.1
C <sub>6</sub> H <sub>10</sub> (cyclohexene)	0.1	0.05
C <sub>5</sub> H <sub>8</sub> (isoprene)	2	2
CH <sub>3</sub> CHO	1	0.5
CH <sub>3</sub> C(O)CH <sub>3</sub>	1	0.5
NO	5	0.025
NO <sub>2</sub>	5	0.025
CO	500 (const.)	100 (const.)
CH <sub>4</sub>	1700 (const.)	1700 (const.)

<sup>a</sup>Units are in ppb.

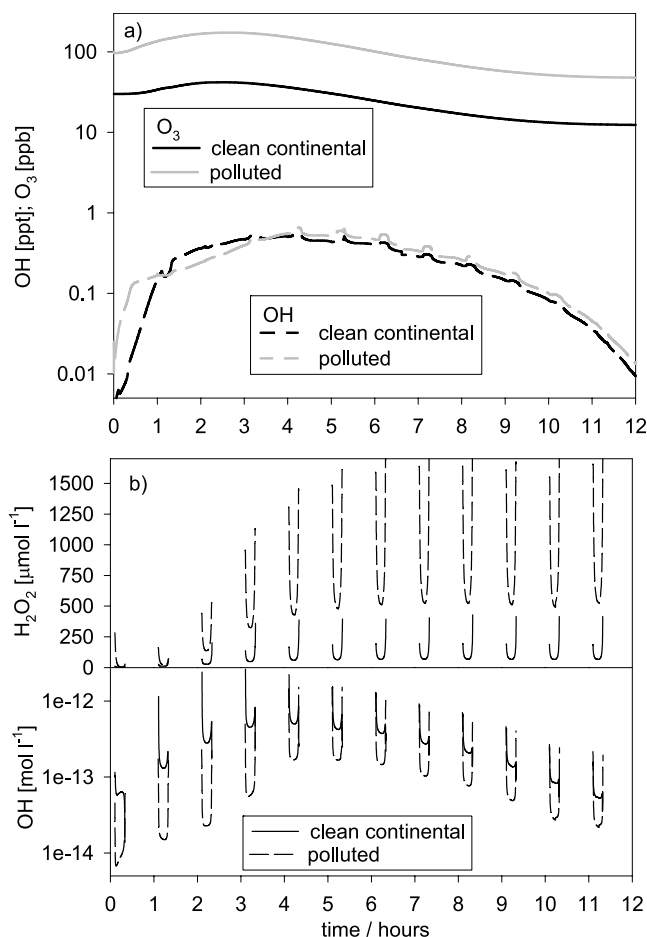


**Figure 6.** Time series of oxidant concentrations. (a) Gas phase concentrations  $O_3$  [ppb] and OH [ppt]. (b) Aqueous phase concentrations  $H_2O_2$  [ $\mu\text{mol l}^{-1}$ ] and OH [ $\text{mol l}^{-1}$ ].

compared to the initial mass. Although the initial concentrations of the organic precursors are of the same order of magnitude as  $SO_2$ , the production of organic aerosol mass is less efficient, and the total organic aerosol mass is about two orders of magnitude lower than that of ammonium sulphate. Sulphate represents the only product in the oxidation of  $SO_2$ , and sulphur(IV) is completely converted to sulphate after a few hours. The product distributions from the oxidation of organics are more diverse. A rough estimate of the conversion efficiency from gas phase precursors to organic aerosol mass formed by the aqueous chemical processes gives a value of less than 50% in the cases studied here. Several volatile species are formed (e.g., HCHO,  $CO_2$ ) as side products not contributing to the aerosol mass (Figures 1–5) so that even assuming the same initial concentration levels for  $SO_2$  and VOC, the absolute aerosol mass formation attributed to organic species is lower. This estimate neglects other processes which contribute to secondary organic aerosol mass, such as partitioning of low volatility gas phase products on aerosol surfaces or new particle formation. Such processes will affect the organic fraction and the organic species distribution in the aerosols. However, these processes and their potential feedback on the physical properties of aerosols are beyond the scope of the present study.

[41] Since for organic species several subsequent oxidation steps are necessary before nonvolatile aerosol components are formed, the rate of organic aerosol mass production is lower than that of sulphate. Thus, in the closed system considered in the present study, it takes about eight cloud cycles until no additional organic mass is formed anymore, while this limit is reached after only three cloud cycles for sulphate.

[42] In the clean continental case the initial  $SO_2$  concentration is 0.01 ppb, leading to only a small increase in the sulphate mass within the first two hours. However, since the selected initial conditions for some organic precursors are similar for the clean continental and polluted cases, the relative increase of the organic mass in the clean continental case is much more significant, with the final total organic mass being about 40% of the final ammonium sulphate mass. Under clean continental conditions, i.e., with lower initial concentrations of  $SO_2$  and some precursor organics, the absolute additional aerosol mass is smaller than in the polluted case. However, relative to the initial mass in the clean continental case the organic chemistry adds about 50% additional mass, while the additional contribution of sulphate mass is less than 15%.

[43] These results show that under both polluted and clean continental conditions organic aqueous phase chemistry can efficiently produce aerosol mass. In both cases the hourly

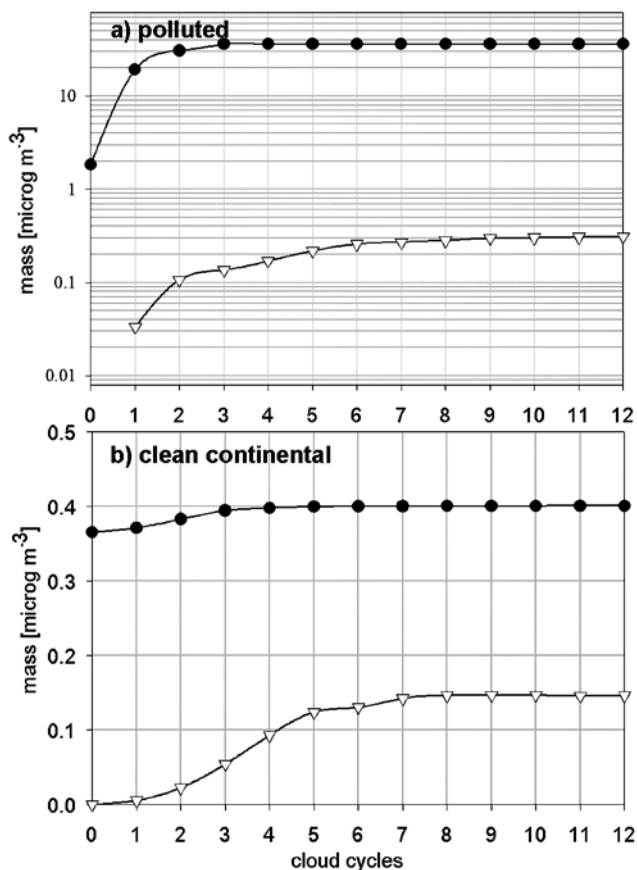


**Figure 7.** Total ammonium sulphate (solid circles) and organic (open triangles) mass [ $\mu\text{g m}^{-3}$ ] in polluted and clean continental conditions. (a) Polluted case (logarithmic scale); (b) clean continental case (linear scale).

**Table 5.** Masses of Organics and Additional Sulphate and Mass Ratios of Sulphate and Organics for Individual Particles ( $m_{\text{single}}$ ) and in Each Size Class ( $m_{\text{class}}$ ) in the Third to Tenth Size Classes After Eight Cloud Cycles<sup>a</sup>

Size Class n	$N$ , $\text{cm}^{-3}$	$r_{\text{dry}}$	$r_{\text{dry}}$	m(Sulphate)		m(nth)/m(3rd)	m(Organics)		m(nth)/m(3rd)	$\frac{m(\text{Sulphate})}{m(\text{Organics})}$	$V_{\text{max}}$ , $\mu\text{m}^3$	$V(\text{nth})/V(3\text{rd})$
		Initial, $\mu\text{m}$	Proc., $\mu\text{m}$	$m_{\text{single}}/10^{-10} \mu\text{g}$	$m_{\text{class}}/\mu\text{g}/\text{m}^3$		$m_{\text{single}}/10^{-10} \mu\text{g}$	$m_{\text{class}}/\mu\text{g}/\text{m}^3$		m(Organics)		
<i>Polluted</i>												
3	65	0.029	0.20	490	3.2	1.0	6.5	0.042	1.0	75	582	1.0
4	186.5	0.048	0.22	730	13.6	1.5	7.3	0.137	1.1	100	629	1.1
5	173.5	0.080	0.23	8.90	15.4	1.9	7.8	0.135	1.2	114	658	1.1
6	52.0	0.13	0.26	1100	5.7	2.3	8.6	0.045	1.3	127	697	1.2
7	5.0	0.22	0.32	1600	0.8	3.3	1.0	$5.0 \cdot 10^{-4}$	1.5	150	792	1.4
8	0.15	0.35	0.45	3400	0.05	6.9	16	$2.4 \cdot 10^{-4}$	2.5	209	1026	1.8
9	$1.7 \cdot 10^{-3}$	0.58	0.65	5600	$9 \cdot 10^{-4}$	11.4	210	$3.5 \cdot 10^{-5}$	32.4	27	6103	10.5
10	$5.5 \cdot 10^{-6}$	0.96	1.00	8600	$5 \cdot 10^{-6}$	17.6	280	$1.5 \cdot 10^{-7}$	43.1	31	8734	15.0
<i>Clean Continental</i>												
3	13	0.029	0.053	3.6	0.0047	1.0	16	0.021	1.0	0.22	3208	1.0
4	37.3	0.048	0.064	3.6	0.013	1.0	17	0.063	1.1	0.21	3140	1.0
5	34.7	0.080	0.088	3.7	0.013	1.0	16	0.055	1.0	0.23	3063	1.0
6	10.4	0.13	0.14	6.1	0.0063	1.7	24	0.025	1.5	0.25	3417	1.1
7	1.0	0.22	0.22	9.0	$9 \cdot 10^{-4}$	2.5	51	0.005	3.2	0.18	7265	2.3
8	0.03	0.35	0.35	9.6	$3 \cdot 10^{-5}$	2.7	41	$1 \cdot 10^{-4}$	2.6	0.24	7708	2.4
9	$3.3 \cdot 10^{-4}$	0.58	0.58	11.0	$4 \cdot 10^{-7}$	3.1	44	$2 \cdot 10^{-7}$	2.8	0.25	8734	2.7
10	$1.1 \cdot 10^{-6}$	0.96	0.96	14.1	$2 \cdot 10^{-9}$	3.9	63	$7 \cdot 10^{-9}$	4.0	0.23	11097	3.5

<sup>a</sup> $V_{\text{max}}$ , maximum volume in each size class at the maximum liquid water content in the eighth cloud cycle;  $m(\text{nth})/m(3\text{rd})$  and  $V(\text{nth})/V(3\text{rd})$  represent the ratio of mass and volume, respectively, between the nth and the third size classes.

production rates are in the range of  $20\text{--}100 \text{ ng m}^{-3} \text{ h}^{-1}$  in the first few hours (assuming a closed system). However, in the polluted scenarios the initial sulphate production rate is about  $20 \mu\text{g m}^{-3} \text{ h}^{-1}$ . These predicted production rates seem to be high compared to absolute masses in atmospheric aerosols. However, these rates represent the maximum rates at the beginning of the simulation time. Average mass production rates for both sulphate and dicarboxylic acids might be of the order of magnitude of a few  $\text{ng m}^{-3} \text{ h}^{-1}$  over the course of a day. Due to the less efficient oxidation of organics in the absence of sunlight and lack of  $\text{H}_2\text{O}_2$  production, the nighttime rates will be much lower. In addition, removal processes of aerosols (deposition) will reduce the total aerosol mass.

#### 4.2. Mass Addition in Different Size Classes

[44] In the current model study we assume an initially pure ammonium sulphate aerosol. However, atmospheric ammonium sulphate particles are generally internally mixed, often with a fairly significant organic fraction [Novakov and Penner, 1993; Quinn and Bates, 2003]. The increase in the total mass as discussed in the previous section shows the efficiency of aqueous phase chemistry for aerosol formation in general. In order to estimate the impact of mass addition by aqueous phase chemistry on subsequent aerosol distributions and finally cloud microphysics, the mass addition in each size class has to be analyzed.

[45] As shown in Figure 7, under polluted conditions the sulphate mass production dominates and significantly exceeds the organic mass production. In Table 5 the mass of additional sulphate (i.e., the difference between the initial and actual sulphate mass) and organic mass are given for the third to tenth size classes after a simulation time of eight hours. Due to the depletion of the precursors, no significant increase in the total mass occurs after about eight cloud cycles. In Figure 8 the resulting dry radii of the individual size classes are shown. The smallest two classes are not

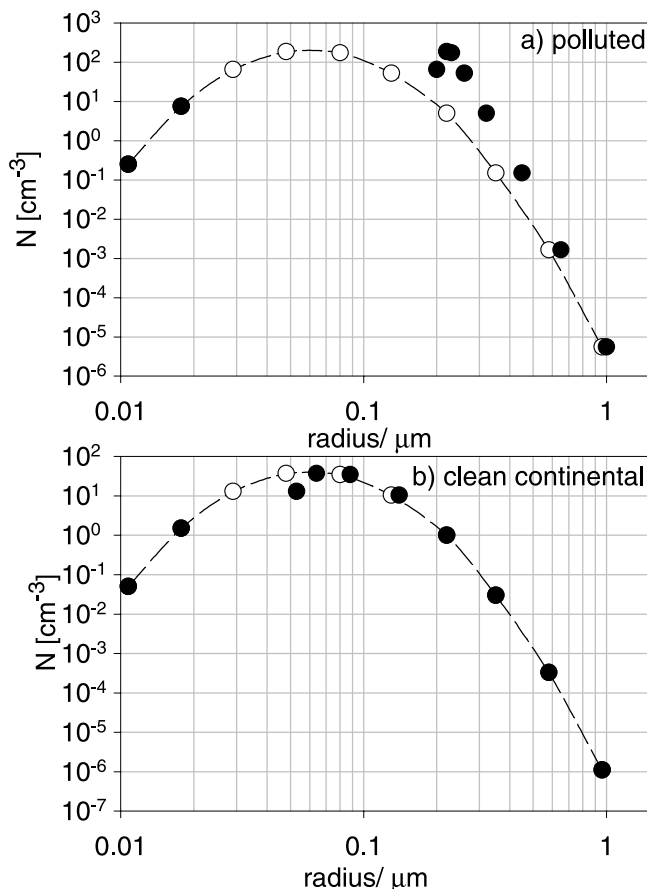


**Figure 8.** Aerosol size distribution. (a) Polluted case; (b) clean continental case. Open circles, initial aerosol; solid circles, processed aerosol after eight cloud cycles.

activated into droplets, and thus their radii are not modified due to aqueous phase chemistry. The most significant change in radii occurs in the third to sixth size classes. Compared to the initial unprocessed aerosol size spectrum the dispersion of the radii of the processed size classes is much narrower. This effect is much more pronounced in the polluted case than in the clean continental case since in the latter case the total mass addition is less effective due to the lower initial precursor concentrations. A similar effect was noted by *Feingold and Kreidenweis* [2000] for sulphate mass addition.

[46] In addition to the masses, in Table 5 we show the drop volume at the time of the highest liquid water content in the eighth cloud cycle. In agreement with previous studies [e.g., *Chameides*, 1984] the increase of the sulphate mass in a particle is correlated with droplet volume. Thus, to a first approximation, the increase in drop volume from the third to the tenth size classes corresponds to an increase in the additional mass. In the polluted case, both sulphate and organic mass production follow this trend in the smaller size classes. However, the organic mass in the two largest size classes exceeds the increase in volume by a factor of three. It should be noted here that the organic mass corresponds to the mass in the aerosol at the end of the cloud cycle and not to the mass in a dry aerosol. Since in the model outgassing processes are not allowed to take place after the total liquid water content falls below  $1 \text{ mg kg}^{-1}$ , independent of the liquid water content in the individual size classes (see Section 2), the large droplets still contain a relatively high amount of water and thus retain some organic species which might evaporate at lower water contents.

#### 4.3. Organic Mass Fraction

[47] While the previous section focused on the formation of the additional aerosol mass in each size class, the resulting chemical modification of the aerosol composition was not addressed. Both the mass addition and the modification of composition determine the microphysical properties of the modified aerosol particles. In Figure 9 the organic fractions of the aerosol particles at the end of a cloud cycle in each size class are shown in hourly time steps. In the polluted case the organic fraction in all size classes does not exceed 3%. There is no clear trend in the distribution of the organic fraction throughout the size classes. After about six hours of simulation time, the organic material accounts for about 1% of the total aerosol mass in all particles.

[48] In the clean continental case there is a significant monotonic decrease of the organic fraction between the third to tenth classes. As seen in Table 5, the absolute additional organic mass does not vary much between the small and large sizes. This mass addition is thus relatively more significant in small particles than in larger ones. In the third and fourth classes the organic mass even exceeds the final ammonium sulphate mass, as reflected by organic fractions of about 65% and 50%, respectively. These size classes account for about 50% of all particles so that the organic fraction of the total mass is significant (Table 5). Given the cited observations that dicarboxylates account for only a small fraction of the total aerosol organic mass, the high [oxalate]/[sulphate] ratio simulated in this case is a result of the very low initial aerosol mass concentration and

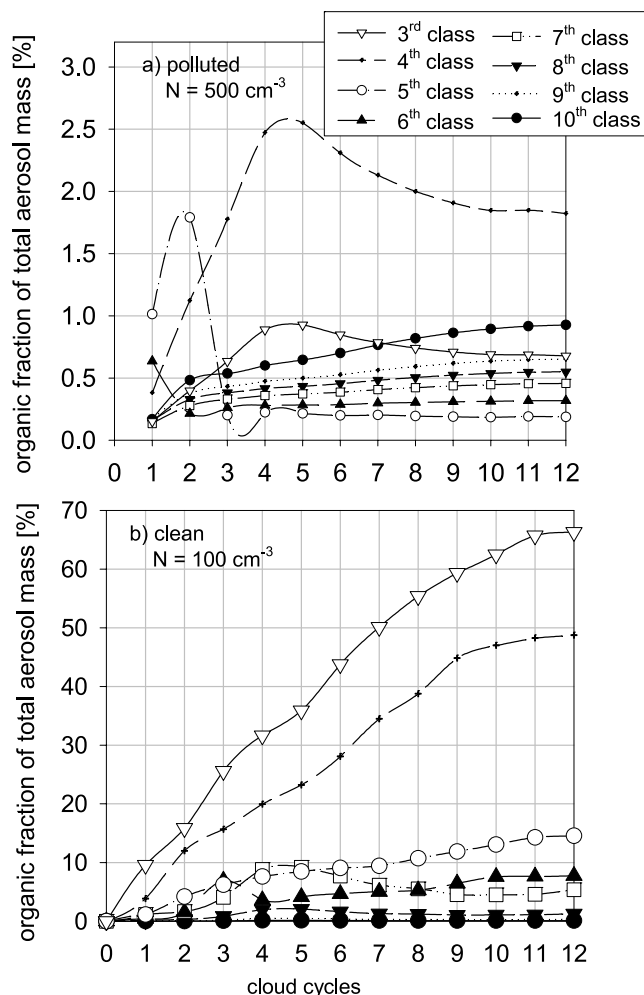


**Figure 9.** Organic fraction (equal to organic mass/(organic mass + ammonium mass + sulfate mass) at the end of each cloud cycle in the third to tenth size class. (a) Polluted case; (b) clean continental case.

the selected initial conditions that lead to minimal sulphur(VI) production.

[49] The pH does not vary much among the size classes. In the polluted case it is between  $2 < \text{pH} < 3$ , while in the clean case it is between  $3.5 < \text{pH} < 4.5$ . Thus, in these moderately acidic droplets, the sulphate production is controlled by the  $\text{H}_2\text{O}_2$  reaction (reaction 4aq, Table 2). The organic mass production is less dependent on pH. In general, the oxidation of undissociated organic acids is slower than that of their corresponding anions [*Karpel vel Leitner and Doré*, 1997; *Ervens et al.*, 2003b], so that according to Figure 5 the loss of organic mass might be decelerated at low pH.

#### 4.4. Organic Species Distribution

[50] Analyses of aerosol samples show that the composition of the organic fraction can be very complex, consisting of many different species. Nevertheless, the small dicarboxylic acids considered in the present mechanism frequently represent a major fraction of the resolved aerosol organic mass [*Finlayson-Pitts and Pitts*, 2000, and references therein], although they generally do not represent a large

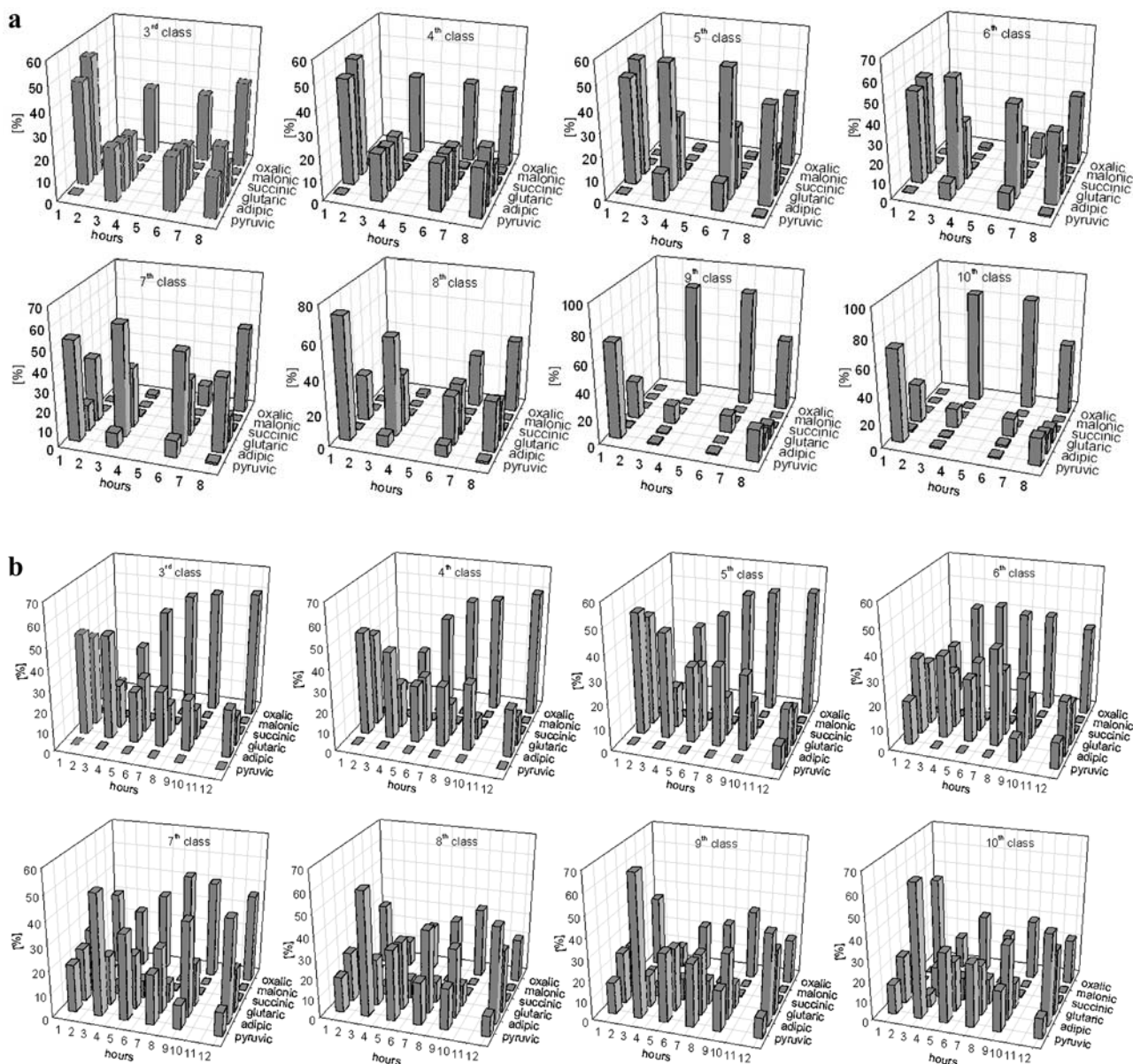


**Figure 10.** Organic species distribution contributing to the organic fraction in (a) polluted conditions (composition shown after first, third, sixth, and eighth cloud cycle) and (b) clean continental conditions (composition shown after first, third, fifth, seventh, ninth, and twelfth cloud cycle).

contribution to the total organic aerosol mass. In laboratory studies it has been shown that different fractions of these species can have quite different influences on the growth of aerosol particles [e.g., *Cruz and Pandis, 2000*].

[51] Figure 10a shows the evolution of the composition of the organic fraction at the end of various cloud cycles for the polluted case. Only the dicarboxylic acids and pyruvic acid are shown since the other possible aerosol constituents (formic, acetic, glyoxylic and glycolic acid) have total contributions of less than 2% due to their high vapor pressures. In the first few hours the organic fractions in the third to sixth size classes are dominated by glutaric and adipic acid, even though their precursor cyclohexene has the smallest initial concentration among the organic precursor species. In the current mechanism the cyclohexene oxidation by OH and O<sub>3</sub> leads to C<sub>5</sub> and C<sub>6</sub> difunctional products

which represent less than 50% of the total carbon (Table 1). Other products are not considered. In contrast to the other pathways leading to the formation of organic aerosol constituents, the oxidation paths of cyclohexene occur in a one step process and lead in this simplified description to nonvolatile aerosol mass. While oxidation of the other precursors also leads to nonvolatile species, it takes a few hours before a significant aerosol mass fraction is accumulated from these precursors. After about six hours the oxalate fraction exceeds that of glutarate and adipate.

[52] There is a significant fraction of pyruvic acid in the larger size classes (7th to 10th), i.e., where more water per droplet is available. Pyruvic acid represents an oxidation product of methylglyoxal, and its only formation pathway in the current mechanism occurs in the aqueous phase. Thus the uptake of this precursor into the droplets seems to limit

the formation of pyruvic acid. In addition, it should be noted that the relative humidity is always >85%, and aqueous phase chemistry occurs if the total liquid water content exceeds  $1 \text{ mg kg}^{-1}$ . For the conditions represented in Figures 10a–10b, all particles still contain some water, and the amount of water in the large particles is relatively high, enhancing the likelihood that more volatile species such as pyruvic acid might be retained in those particles.

[53] It can be seen in Figure 10a (polluted case) that the decay of pyruvic acid is quite rapid, and its fraction is negligible after a few hours. Comparing the rate constants in Table 2, it becomes evident that the oxidation of pyruvic acid (R-21aq) is much faster than the corresponding processing of oxalic acid (R-18aq and R-20aq). The large size classes do not contribute significantly to the total number of particles (Figure 8), so that the pyruvic acid fractions are negligible in the total organic fraction of the internally mixed aerosol distribution.

[54] The relative distributions of organic species in the clean continental case (Figure 10b) are very similar to those in the polluted case. Here, too, the fraction of oxalic acid increases monotonically until about half of the organic material consists of oxalic acid. This is expected, since oxalate represents an end product in the oxidation chain of all gas phase precursors considered here (Figure 5). However, in the larger size classes the oxalate fraction decreases in the last hours, accounting for a possible decrease in total organic mass. Oxidation of oxalate causes potentially a significant decrease in organic mass (Figure 5). Decay of the higher dicarboxylic acids causes the molar mass to diminish by only  $14 \text{ g mol}^{-1}$  (the loss of the internal  $\text{CH}_2$  group; Figure 4). However, the oxidation of oxalic acid leads to the complete conversion of organic carbon to  $\text{CO}_2$  which volatilizes. The relative increase of the glutarate/adipate masses (in the seventh and eighth class) at the end of the simulation results from decreases in the masses of pyruvic and oxalic acid.

[55] The high fraction of oxalate within the organic fraction simulated here is in agreement with observations. In several studies it has been shown that the mass of oxalate exceeds the masses of other dicarboxylic acids [Neusüß *et al.*, 2000]. While oxalic acid seems to be ubiquitous in aerosol samples, the data sets for pyruvic acid are much sparser. In continental areas pyruvic acid concentrations are quite variable, a few  $\text{ng m}^{-3}$  up to a few  $\mu\text{g m}^{-3}$  [Talbot *et al.*, 1995]. In very clean (marine) conditions, pyruvic acid concentrations do not exceed values of  $10 \text{ ng m}^{-3}$  [Baboukas *et al.*, 2000].

#### 4.5. Comparison With Observations: Mass Production and Mass Ratio of Dicarboxylate to Ammonium Sulfate

[56] Observations show that the sulphate concentrations in particles under polluted conditions are much higher than in remote areas. In fact, in polluted continental regions sulphate concentrations of up to a few hundred  $\mu\text{g m}^{-3}$  have been observed, while in remote areas they are usually smaller by up to three orders of magnitude [Finlayson-Pitts and Pitts, 2000]. In comparison, measurements of dicarboxylic acid concentrations in clean and polluted scenarios differ much less. In the urban atmosphere during summer, concentrations of  $\leq 1000 \text{ ng m}^{-3}$  [Kawamura and Kaplan, 1987; Kawamura and Ikushima, 1993] were found, while

over the ocean aerosol samples reveal concentrations of  $\leq 150 \text{ ng m}^{-3}$  [Mochida *et al.*, 2003a].

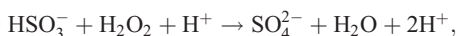
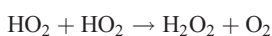
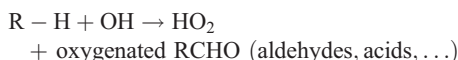
[57] The ratios of dicarboxylate mass to ammonium sulphate mass predicted from the current model study are about 0.01 for the polluted, and about 0.3 for the clean continental case, respectively (Figure 7). While the absolute masses of both sulphate and dicarboxylic acids are in broad agreement with observations, the mass ratio of [dicarboxylates]/[sulphate] predicted by the model is quite high compared to observations in different environments. As discussed previously, the dicarboxylate mass predicted by our model study represents an upper limit due to the omission of many other physical and chemical processes.

[58] In marine and remote scenarios oxalate mass (the dominant proxy for dicarboxylic acid) is about one order of magnitude lower than the sulphate mass in the same samples [Collett *et al.*, 1999; Mochida *et al.*, 2003a, 2003b]. In a semirural environment Edney *et al.* [2003] determined a ratio [oxalate]/[sulphate] < 0.04. In more polluted (urban) scenarios mass ratios in the range of 0.005–0.04 were observed [Khwaja *et al.*, 1995; Kerminen *et al.*, 2000]. In more continental scenarios the mass ratio of [oxalate]/[sulphate] is smaller due to the higher fraction of less oxygenated organics to the total organic material [Kawamura and Ikushima, 1993; Sempéré and Kawamura, 1996] and thus a lower contribution of dicarboxylic acids to the total organic carbon [Kerminen *et al.*, 2000; Kawamura *et al.*, 2003]. Very high mass ratios of  $0.15 < [\text{oxalate}]/[\text{sulphate}] < 0.33$  were observed by Ruellan *et al.* [1999] in scenarios which were strongly influenced by forest fires. However, under such conditions it is likely that different pathways are responsible for the aerosol mass formation, and such scenarios are not comparable to the previously mentioned studies.

[59] Observations in continental areas reveal organic fractions of about 20–50% of the total aerosol mass in aerosol particles [Saxena and Hildemann, 1996]. In general, dicarboxylic acids have been found to account for only small percentages of the total organic aerosol mass [Khwaja *et al.*, 1995; Mochida *et al.*, 2003b], so the predictions from this simulation are in qualitative agreement with observations. Indeed, the organic fraction of urban aerosols is largely composed of hydrophobic, i.e., less oxygenated species, which are not considered in the current model. Nevertheless, other model assumptions that affect the predicted percentage contributions, must be clarified. First, and most importantly, the choice of initial conditions for the aerosol mass concentration, available  $\text{SO}_2$ , and available oxidants enhances the importance of the sulphur(VI) production in this simulation, as discussed previously. Further, the closed system assumed here ignores emission strengths. Fresh emissions enable a continuous renewal of precursor concentrations so that organic mass may be formed more efficiently. It is likely that other or additional sources for dicarboxylic acids, such as the direct emissions from exhaust or additional heterogeneous processes, might contribute to their mass. In addition, aerosol losses by deposition will change the aerosol mass; however, such processes are not included in the model.

[60] The present model study investigates only two sets of initial concentrations representing two different and

somewhat extreme scenarios. The computed mass ratios of [dicarboxylates]/[sulphate] are a direct consequence of the choice of initial conditions, particularly for the initial aerosol and SO<sub>2</sub> concentrations, and could be readily adjusted by modifying the initial concentrations. However, besides the direct influence on the aerosol mass production rates, changing values of the initial parameters will cause a feedback to the production rates. For example, due to the following reaction cycle, the oxidation of organics might enhance the efficiency of sulphate production:



where R – H represents any organic species either in the gas or aqueous phase. In addition, gas phase oxidation of organics leads to higher ozone concentration levels. At higher pH values, in the aqueous phase ozone might enhance sulphate formation as well.

[61] The sensitivity of the mass production rates to the reaction chain above and other complex feedbacks of the HO<sub>x</sub>-NO<sub>x</sub> cycles are included in this model but are not analyzed explicitly here since their influence on each other will be different for every initial set of conditions. As mentioned before there are still significant gaps of knowledge in the chemical mechanism development with respect to organics (in particular in the aqueous phase), so that the possibility that additional loss processes of the organic aerosol constituents occur cannot be excluded. In addition, we have assumed for the current model study that the dicarboxylic acids are not volatile. This assumption might represent another reason for an overestimate of dicarboxylic acid mass in the particles since recent measurements have shown that at relative humidities of about 80%, up to 30% of oxalic acid might be present in the gas phase [Baboukas *et al.*, 2000]. The partitioning of the dicarboxylic acids between gas and aerosol phases will depend strongly on the phase of the aerosol, acidity, and temperature.

[62] In addition, we have neglected the photolysis of carboxylic acids in the aqueous phase. However, we have estimated, based on data by Faust *et al.* [1997], that the photolysis of pyruvic acid will be a negligible loss process under these conditions. Iron-dicarboxylato-complexes are photolabile. Many observations have revealed that the iron fraction in sulphate particles (or internally mixed sulphate/organics particles) is usually very low [Murphy and Thomson, 1997a, 1997b]. Zuo and Hoigné [1992] report a photolysis rate of  $3.7 \cdot 10^{-9} \text{ M s}^{-1}$  for the iron-oxalato-complex. They assumed aqueous phase concentrations of 1 μM and 5 μM for iron and oxalate, respectively. Based on these values the natural lifetime  $\tau$  for oxalate is  $\sim 650 \text{ s}$ , which is even less than the lifetime of one cloud under our model conditions. Thus the oxalate concentration predicted by our model represents an upper limit and might be lower if iron-oxalato-complexes are present. The influence on the other dicarboxylates is probably weaker, as shown by Faust

and Zepp [1993], who predicted that the half-life of the malonato-complex is a factor of 25 higher than that of the oxalato-complex.

## 5. Conclusions

[63] While previous studies have focused on the importance of aqueous production of sulphate particulate matter, the current study extends this idea by considering organic mass production in a size resolved aerosol model. A chemical mechanism focusing on the formation of dicarboxylic acids in cloud drops has been developed. The effect of chemical in-cloud processes on the generation of secondary organic aerosol mass has been analyzed. It has been shown that oxidation of organic species does not produce aerosol mass as efficiently as does oxidation of sulphur(IV), in part because in the latter case all sulphur(VI) is nonvolatile, whereas many additional volatile and nonvolatile products might be formed in the gas and aqueous phase by oxidation of organic species. Nevertheless, for the initial conditions chosen here, the total organic aerosol mass formed in both polluted and clean continental conditions is about 100–300 ng m<sup>-3</sup> after a simulation time of 12 hours. These absolute masses are in general agreement with results of analyses of aerosol samples. The simulated relative magnitudes of sulphate and organic mass in the modified aerosols are dependent on the assumed initial conditions. In addition, the consideration of different precursor compounds and/or additional chemical production/loss pathways may also lead to different production rates for these compounds. The net production rates for organic aerosol mass in this model study represent upper limits since limitations of the chemical mechanism result in the neglect of various loss processes. In addition, formation of more volatile organic compounds, which do not contribute to organic mass formation in clouds, might influence the oxidant concentration levels in the gas phase. Adsorption onto the particle phase or heterogeneous surface processes might contribute to the organic aerosol mass and influence the microphysical behaviour of the aerosols. Less hygroscopic organics which are adsorbed onto particle surfaces may form a separate condensed organic phase and thus do not contribute to any chemical processes in the aqueous phase. Because the surface area of droplets is a few orders of magnitude larger than that of dry particles, the uptake on droplets represents a more efficient sink for soluble low volatility species (e.g., dicarboxylic acids) as long as droplets are present.

[64] The chemical mechanism presented here is restricted to a few organic precursors representing classes of major emission such as aromatics, alkenes and terpenes. It can be expected that other species within these classes might be efficiently oxidized and contribute to organic aerosol mass. The current mechanism treats only the formation of dicarboxylic acids  $\leq \text{C}_6$  by aqueous phase processes, but the mass ranges for these species predicted by the current model are in broad agreement with observations. Longer acids in aerosol particles are likely to be formed by other chemical processes such as heterogeneous surface reactions [Moise and Rudich, 2002; Eliason *et al.*, 2003] which are currently not considered.

[65] The relative contributions of particular organic compounds to the total dicarboxylate mass are similar in the polluted and clean continental cases considered here. In both scenarios glutaric, adipic, oxalic and pyruvic acids dominate. High concentrations of oxalic acid, relative to those of other dicarboxylic acids, at the end of the simulation reflect its role as the end product of several organic oxidation chains in cloud droplets. The present study allows identification of the direct precursors of glutaric and adipic acid, but the precursor identification is more difficult and less clearly defined for other species, such as oxalic acid originating from several oxidation chains. These results are in qualitative agreement with observations: of the species comprising the total aerosol organic mass that have been resolved to date, glutaric acid represents a major secondary species [Cruz and Pandis, 1998], and oxalic acid has been identified as the largest single resolved contributor to the organic mass [e.g., Neusüß et al., 2000; Lee et al., 2002, 2003].

[66] In the current model the aerosol size distribution is only changed by the addition of newly formed organic and sulphate mass. The treatment of the water uptake by these internally mixed organic/sulphate aerosols was simplified since the hygroscopic properties of the dissolved organic mass were assumed to be the same as those for ammonium (bi-)sulphate/sulphuric acid. However, it is known from several recent laboratory studies that significant fractions of dicarboxylic acids in ammonium sulphate particles might change the particles' hygroscopic behavior [Cruz and Pandis, 2000; Brooks et al., 2002; Prenni et al., 2003]. The extent of these deviations depends on the amount and composition of the organic fraction and may lead to a different water distribution throughout the aerosol size classes. This variation in water content may in turn lead to modified droplet sizes, which might then influence the uptake rates of reactive species into the aqueous phase. Part 2 of this series will focus on a more detailed investigation of the microphysical properties of organic and internally mixed inorganic/organic aerosols [Ervens et al., 2004], clarifying the extent to which the simplified assumptions about the hygroscopicity of organics might be appropriate and under which conditions dicarboxylic acids might have a significant influence on the microphysical behavior of aerosol particles.

[67] **Acknowledgments.** This work was supported by the NOAA Office of Global Programs. We thank two anonymous reviewers for their valuable suggestions and comments.

## References

- Anttila, T., and V.-M. Kerminen (2003), Aerosol formation via aqueous-phase chemical reactions, *J. Geophys. Res.*, *108*(D4), 4134, doi:10.1029/2002JD002764.
- Aschmann, S. M., E. C. Tuazon, J. Arey, and R. Atkinson (2003), Products of the gas-phase reaction of O<sub>3</sub> with cyclohexene, *J. Phys. Chem. A*, *107*, 2247–2255.
- Atkinson, R. (1986), Kinetics and mechanisms of the gas-phase reactions of the hydroxyl radical with organic compounds under atmospheric conditions, *Chem. Rev.*, *86*, 69.
- Atkinson, R., D. L. Baulch, R. A. Cox, R. F. Hampson Jr., J. A. Kerr, M. J. Rossi, and J. Troe (1997), Evaluated kinetic, photochemical, and heterogeneous data for atmospheric chemistry: Supplement V, IUPAC subcommittee on gas kinetic data evaluation for atmospheric chemistry, *J. Phys. Chem. Ref. Data*, *26*, 521–1011.
- Baboukas, E. D., M. Kanakidou, and N. Mihalopoulos (2000), Carboxylic acids in gas and particulate phase above the Atlantic Ocean, *J. Geophys. Res.*, *105*(D11), 14,459–14,471.
- Bacher, C., G. S. Tyndall, and J. J. Orlando (2001), The atmospheric chemistry of glycolaldehyde, *J. Atmos. Chem.*, *39*, 171–189.
- Beilke, S., and G. Gravenhorst (1978), Heterogeneous SO<sub>2</sub>-oxidation in the droplet phase, *Atmos. Environ.*, *12*, 231–239.
- Betterton, E. A., and M. R. Hoffmann (1988), Henry's law constants of some environmentally important aldehydes, *Environ. Sci. Technol.*, *22*, 1415–1418.
- Blando, J. D., and B. J. Turpin (2000), Secondary organic aerosol formation in cloud and fog droplets: A literature evaluation of plausibility, *Atmos. Environ.*, *34*, 1623–1632.
- Brooks, S. D., M. E. Wise, M. Cushing, and M. A. Tolbert (2002), Deliquescence behavior of organic/ammonium sulfate aerosol, *Geophys. Res. Lett.*, *29*(19), 1917, doi:10.1029/2002GL014733.
- Chameides, W. L. (1984), Photochemistry of a remote marine stratiform cloud, *J. Geophys. Res.*, *89*, 4739–4755.
- Chameides, W. L., and A. W. Stelson (1992), Aqueous phase chemical processes in deliquescent sea-salt aerosols: A mechanism that couples the atmospheric cycles of S and sea salt, *J. Geophys. Res.*, *97*(D5), 20,565–20,580.
- Chameides, W. L., et al. (1992), Ozone precursor relationships in the ambient atmosphere, *J. Geophys. Res.*, *97*(D5), 6037–6055.
- Chebbi, A., and P. Carlier (1996), Carboxylic acids in the troposphere, occurrence, sources, and sinks: A review, *Atmos. Environ.*, *30*(24), 4233–4249.
- Collett, J. L., K. J. Hoag, D. E. Sherman, A. Bator, and L. W. Richards (1999), Spatial and temporal variations in San Joaquin Valley fog chemistry, *Atmos. Environ.*, *33*, 129–140.
- Corrigan, C. E. (2001), The ability of organic compounds to behave as cloud condensation nuclei, Ph.D. thesis, Univ. of Calif., Berkeley.
- Cruz, C. N., and S. N. Pandis (1998), The effect of organic coatings on the cloud condensation nuclei activation of inorganic atmospheric aerosol, *J. Geophys. Res.*, *103*(D11), 13,111–13,123.
- Cruz, C. N., and S. N. Pandis (2000), Deliquescence and hygroscopic growth of mixed inorganic-organic atmospheric aerosols, *Environ. Sci. Technol.*, *34*, 4313–4319.
- DeBruyn, W. J., E. Swartz, J. H. Hu, J. A. Shorter, P. Davidovits, D. R. Worsnop, M. S. Zahniser, and C. E. Kolb (1995), Henry's law solubilities and Setchenow coefficients for biogenic reduced sulphur species obtained from gas-liquid uptake measurements, *J. Geophys. Res.*, *100*(D4), 7245–7251.
- Dixon, R. W., and H. Aasen (1999), Measurement of hydroxymethanesulfonate in atmospheric aerosols, *Atmos. Environ.*, *33*, 2023–2029.
- Edney, E. O., T. E. Kleindienst, T. S. Conner, C. D. McIver, E. W. Corse, and W. S. Weathers (2003), Polar organic oxygenates in PM<sub>2.5</sub> at a southeastern site in the United States, *Atmos. Environ.*, *37*, 3947–3965.
- Eliason, T. L., S. Aloisio, D. J. Donaldson, D. J. Czizco, and V. Vaida (2003), Processing of unsaturated organic acid films and aerosols by ozone, *Atmos. Environ.*, *37*, 2207–2219.
- Ervens, B. (2001), Troposphärische Multiphasenchemie: Modellrechnungen und kinetische Untersuchungen des OH-Radikals in wässriger Lösung, Ph.D. thesis, Univ. of Leipzig, Leipzig, Germany.
- Ervens, B., et al. (2003a), CAPRAM2.4 (MODAC mechanism): An extended and condensed tropospheric aqueous phase mechanism and its application, *J. Geophys. Res.*, *108*(D14), 4426, doi:10.1029/2002JD002202.
- Ervens, B., S. Gligorovski, and H. Herrmann (2003b), Temperature-dependent rate constants for hydroxyl radical reactions with organic compounds in aqueous solution, *Phys. Chem. Chem. Phys.*, *5*, 1811–1824.
- Ervens, B., G. Feingold, S. L. Clegg, and S. M. Kreidenweis (2004), A modeling study of aqueous production of dicarboxylic acids: 2. Implications for cloud microphysics, *J. Geophys. Res.*, *109*, D15206, doi:10.1029/2004JD004575.
- Facchini, M. C., M. Mircea, S. Fuzzi, and R. J. Charlson (1999), Cloud albedo enhancement by surface-active organic solutes in growing droplets, *Nature*, *401*, 257–259.
- Faust, B. C., and R. G. Zepp (1993), Photochemistry of aqueous iron(III)-polycarboxylate complexes: Roles in the chemistry of atmospheric and surface waters, *Environ. Sci. Technol.*, *27*, 2517–2522.
- Faust, B. C., K. Powell, C. J. Rao, and C. Anastasio (1997), Aqueous-phase photolysis of biacetyl (an  $\alpha$ -dicarbonyl compound): A sink for biacetyl, and a source for acetic acid, peroxyacetic acid, hydrogenperoxide, and the highly oxidizing acetylperoxy radical in aqueous aerosols, fogs, and clouds, *Atmos. Environ.*, *31*, 497–510.
- Feingold, G., and A. J. Heymsfield (1992), Parameterizations of condensational growth of droplets for use in general circulation models, *J. Aerosol Sci.*, *49*, 2325–2342.

- Feingold, G., and S. M. Kreidenweis (2000), Does cloud processing of aerosol enhance droplet concentrations?, *J. Geophys. Res.*, *105*(D19), 24,351–24,361.
- Feingold, G., and S. M. Kreidenweis (2002), Cloud processing of aerosol as simulated by a Large Eddy Simulation with coupled microphysics and aqueous chemistry, *J. Geophys. Res.*, *107*(D23), 4687, doi:10.1029/2002JD002054.
- Feingold, G., S. M. Kreidenweis, and Y. Zhang (1998), Stratocumulus processing of gases and cloud condensation nuclei: 1. Trajectory ensemble model, *J. Geophys. Res.*, *103*(D16), 19,527–19,542.
- Finlayson-Pitts, B., and J. N. Pitts Jr. (2000), *Chemistry of the Upper and Lower Atmosphere: Theory, Experiments, and Applications*, Academic, San Diego, Calif.
- Forstner, H. J. L., R. C. Flagan, and J. H. Seinfeld (1997), Secondary organic aerosol from the photooxidation of aromatic hydrocarbons: Molecular composition, *Environ. Sci. Technol.*, *31*, 1345–1358.
- Frost, G. J., et al. (1998), Photochemical ozone production in the rural southeastern United States during the 1990 Rural Oxidants in the Southern Environment (ROSE) program, *J. Geophys. Res.*, *103*(D17), 22,491–22,508.
- Gierczak, T., J. B. Burkholder, R. K. Talukdar, A. Mellouki, S. B. Barone, and A. R. Ravishankara (1997), Atmospheric fate of methyl vinyl ketone and methacrolein, *J. Photochem. Photobiol. A*, *110*, 1–10.
- Goldan, P. D., W. C. Kuster, F. C. Fehsenfeld, and S. A. Montzka (1995), Hydrocarbon measurements in the southeastern United States: The Rural Oxidants in the Southern Environment (ROSE) program 1990, *J. Geophys. Res.*, *100*(D12), 25,945–25,963.
- Goldan, P. D., D. D. Parrish, W. C. Kuster, M. Trainer, S. A. McKeen, J. Holloway, B. T. Jobson, D. T. Sueper, and F. C. Fehsenfeld (2000), Airborne measurements of isoprene, CO, and anthropogenic hydrocarbons and their implications, *J. Geophys. Res.*, *105*(D7), 9091–9105.
- Graedel, T. E., and C. J. Weschler (1981), Chemistry within aqueous atmospheric aerosols and raindrops, *Rev. Geophys.*, *19*, 505–539.
- Griffin, R. J., D. Dabdub, and J. H. Seinfeld (2002), Secondary organic aerosol: 1. Atmospheric chemical mechanism for production of molecular constituents, *J. Geophys. Res.*, *107*(D17), 4332, doi:10.1029/2001JD000541.
- Grosjean, D., E. L. Williams, and E. Grosjean (1993), Atmospheric chemistry of isoprene and of its carbonyl products, *Environ. Sci. Technol.*, *27*, 830–840.
- Grosjean, E., D. J. Grosjean, and J. H. Seinfeld (1996), Atmospheric chemistry of 1-octene, 1-decene, and cyclohexene: Gas-phase carbonyl and peroxyacyl nitrate products, *Environ. Sci. Technol.*, *30*, 1038–1047.
- Hatakeyama, S., T. Tanonaka, J. Weng, H. Bandow, H. Takagi, and H. Akimoto (1985), Ozone-cyclohexene reaction in air: Quantitative analysis of particulate products and the reaction mechanism, *Environ. Sci. Technol.*, *19*, 935–942.
- Hegg, D. A., R. Majeed, P. F. Yuen, M. B. Baker, and T. V. Larson (1996), The impact of SO<sub>2</sub> oxidation in cloud droplets and in haze particles on aerosol light scattering and CCN activity, *Geophys. Res. Lett.*, *23*, 2613–2626.
- Herrmann, H. (2003), Kinetics of aqueous phase reactions relevant for atmospheric chemistry, *Chem. Rev.*, *103*(12), 4691–4716.
- Herrmann, H., B. Ervens, H.-W. Jacobi, R. Wolke, P. Nowacki, and R. Zellner (2000), CAPRAM2.3: A chemical aqueous phase radical mechanism for tropospheric chemistry, *J. Atmos. Chem.*, *38*, 231–284.
- Hoffmann, M. R. (1986), On the kinetics and mechanism of oxidation of aquated sulfur dioxide by ozone, *Atmos. Environ.*, *20*, 1145–1154.
- Iraci, L. T., B. M. Baker, G. S. Tyndall, and J. J. Orlando (1998), Measurements of the Henry's law coefficients of 2-methyl-3-butenol, methacrolein, and methylvinyl ketone, *J. Atmos. Chem.*, *33*, 321–330.
- Jang, M., and R. M. Kamens (2001), Atmospheric secondary aerosol formation by heterogeneous reactions of aldehydes in the presence of sulfuric acid aerosol catalyst, *Environ. Sci. Technol.*, *35*, 4758–4766.
- Kalberer, M., J. Yu, D. R. Cocker, R. C. Flagan, and J. H. Seinfeld (2000), Aerosol formation in the cyclohexene-ozone system, *Environ. Sci. Technol.*, *34*, 4894–4901.
- Karpel vel Leitner, N., and M. Doré (1997), Mécanisme d'action des radicaux OH sur les acides glycolique, glyoxylique, acétique et oxalique en solution aqueuse: Incidence sur la consommation de peroxyde d'hydrogène dans le système H<sub>2</sub>O<sub>2</sub>/UV et O<sub>3</sub>/H<sub>2</sub>O<sub>2</sub>, *Water Res.*, *6*, 1383–1397.
- Kawamura, K., and K. Ikushima (1993), Seasonal changes in the distribution of dicarboxylic acids in the urban atmosphere, *Environ. Sci. Technol.*, *27*, 2227–2235.
- Kawamura, K., and I. R. Kaplan (1987), Motor exhaust emissions as primary source for dicarboxylic acids in Los Angeles ambient air, *Environ. Sci. Technol.*, *21*(1), 105–110.
- Kawamura, K., and F. Sakaguchi (1999), Molecular distributions of water-soluble dicarboxylic acids in marine aerosols over the Pacific Ocean including tropics, *J. Geophys. Res.*, *104*(D3), 3501–3509.
- Kawamura, K., N. Umemoto, M. Mochida, T. Bertram, S. Howell, and B. J. Huebert (2003), Water-soluble dicarboxylic acids in the tropospheric aerosols collected over east Asia and western North Pacific by ACE-Asia C-130 aircraft, *J. Geophys. Res.*, *108*(D23), 8639, doi:10.1029/2002JD003256.
- Kerminen, V., C. Ojanen, T. Pakkanen, R. Hillamo, M. Aurela, and J. Meriläinen (2000), Low molecular-weight dicarboxylic acids in an urban and rural atmosphere, *J. Aerosol Sci.*, *31*(3), 349–362.
- Khwaja, H. A., S. Brudnoy, and L. Husain (1995), Chemical characterization of three summer cloud episodes at Whiteface Mountain, *Chemosphere*, *31*, 3357–3381.
- Kumar, P. P., K. Broekhuizen, and J. P. D. Abbatt (2003), Organic acids as cloud condensation nuclei: Laboratory studies of highly soluble and insoluble species, *Atmos. Chem. Phys.*, *3*, 509–520.
- Langner, J., and H. Rodhe (1991), A global three-dimensional model of the tropospheric sulfur-cycle, *J. Atmos. Chem.*, *13*, 225–263.
- Lee, S., D. M. Murphy, D. S. Thomson, and A. M. Middlebrook (2002), Chemical components of single particles measured with Particle Analysis by Laser Mass Spectrometry (PALMS) during the Atlanta Super Site Project: Focus on organic/sulfate, lead, soot, and mineral particles, *J. Geophys. Res.*, *107*(D1), 4003, doi:10.1029/2000JD000011.
- Lee, S., D. M. Murphy, D. S. Thomson, and A. M. Middlebrook (2003), Nitrate and oxidized organic ions in single particle mass spectra during the 1999 Atlanta Supersite Project, *J. Geophys. Res.*, *108*(D7), 8417, doi:10.1029/2001JD001455.
- Lide, D. R. (Ed.) (2000), *Handbook of Chemistry and Physics*, 83rd ed., CRC Press, Boca Raton, Fla.
- Lightfoot, P. D., R. A. Cox, J. N. Crowley, M. Destriau, G. D. Hayman, M. E. Jenkin, G. K. Moortgat, and F. Zabel (1992), Organic peroxy radicals: Kinetics, spectroscopy, and tropospheric chemistry, *Atmos. Environ.*, *Part A*, *26*, 1805–1961.
- Logan, S. R. (1989), Redox reactions of organic radicals with ferrocenyl/ferricenium species in aqueous solution: Part 1: Radical derived from carboxylic acids, *J. Chem. Soc. Perkin Trans.*, *2*, 751–754.
- Madronich, S. (1987), Photodissociation in the atmosphere: 1. Actinic flux and the effects of ground reflections and clouds, *J. Geophys. Res.*, *92*, 9740–9752.
- Madronich, S. (1993), UV radiation in the natural and perturbed atmosphere, in *Environmental Effects of UV (Ultraviolet) Radiation*, edited by M. Tevini, pp. 17–69, Lewis, Boca Raton, Fla.
- Mochida, M., N. Umemoto, K. Kawamura, and M. Uematsu (2003a), Bimodal size distribution of C<sub>2</sub>-C<sub>4</sub> dicarboxylic acids in the marine aerosols, *Geophys. Res. Lett.*, *30*(13), 1672, doi:10.1029/2003GL017451.
- Mochida, M., K. Kawamura, N. Umemoto, M. Uematsu, M. Kobayashi, S. Matsunaga, H.-J. Lim, B. J. Turpin, T. S. Bates, and B. R. T. Simoneit (2003b), Spatial distributions of oxygenated organic compounds (dicarboxylic acids, fatty acids, and levoglucosan) in marine aerosols over the western Pacific and off the coast of East Asia: Continental outflow of organic aerosols during the ACE-Asia campaign, *J. Geophys. Res.*, *108*(D23), 8638, doi:10.1029/2002JD003249.
- Moise, T., and Y. Rudich (2002), Reactive uptake of ozone by aerosol-associated unsaturated fatty acids: Kinetics, mechanism, and products, *J. Phys. Chem. A*, *106*, 6469–6476.
- Moortgat, G. K., B. Veyret, and R. Lesclaux (1989), Kinetics of the reaction of HO<sub>2</sub> with CH<sub>3</sub>C(O)O<sub>2</sub> in the temperature range 253–368 K, *Chem. Phys. Lett.*, *160*, 443–448.
- Murphy, D. M., and D. S. Thomson (1997a), Chemical composition of single aerosol particles at Idaho Hill: Positive ion measurements, *J. Geophys. Res.*, *102*(D5), 6341–6352.
- Murphy, D. M., and D. S. Thomson (1997b), Chemical composition of single aerosol particles at Idaho Hill: Negative ion measurements, *J. Geophys. Res.*, *102*(D5), 6353–6368.
- Neusüß, C., M. Pelzing, A. Plewka, and H. Herrmann (2000), A new analytical approach for size-resolved speciation of organic compounds in atmospheric aerosol particles: Methods and first results, *J. Geophys. Res.*, *105*(D4), 4513–4527.
- Niki, H., P. D. Maker, C. M. Savage, and L. P. Breitenbach (1981), An FTIR study of mechanisms for the HO radical initiated oxidation of C<sub>2</sub>H<sub>4</sub> in presence of NO: Detection of glycolaldehyde, *Chem. Phys. Lett.*, *80*, 499–503.
- Novakov, T., and J. E. Penner (1993), Large contributions of organic aerosols to cloud-condensation-nuclei concentrations, *Nature*, *365*, 823–826.
- Odum, J. R., T. Hoffmann, F. Bowman, D. Collins, R. C. Flagan, and J. H. Seinfeld (1996), Gas/particle partitioning and secondary organic aerosol yields, *Environ. Sci. Technol.*, *30*, 2580–2585.
- Peng, C., M. Chang, and C. K. Chang (2001), The hygroscopic properties of dicarboxylic and multifunctional acids: Measurements and UNIFAC predictions, *Environ. Sci. Technol.*, *35*, 4495–4501.
- Pitzer, K. S. (1991), Ion interaction approach: Theory and data correlation, in *Activity Coefficients in Electrolyte Solutions*, edited by K. S. Pitzer, CRC Press, Boca Raton, Fla.

- Pöschl, U., R. v. Kuhlmann, N. Poisson, and P. J. Crutzen (2000), Development and intercomparison of condensed isoprene oxidation mechanisms for global atmospheric modelling, *J. Atmos. Chem.*, *37*, 29–52.
- Prenni, A. J., P. DeMott, S. M. Kreidenweis, and D. E. Sherman (2001), The effects of low molecular weight dicarboxylic acids on cloud formation, *J. Phys. Chem. A*, *105*, 11,240–11,248.
- Prenni, A. J., P. J. DeMott, and S. M. Kreidenweis (2003), Water uptake and ice nucleation of internally mixed particles containing ammonium sulfate and dicarboxylic acids, *Atmos. Environ.*, *37*, 4243–4251.
- Pun, B. K., C. Seigneur, D. Grosjean, and P. Saxena (2000), Gas-phase formation of water-soluble organic compounds in the atmosphere: A retrosynthetic analysis, *J. Atmos. Chem.*, *35*, 199–223.
- Quinn, P., and T. Bates (2003), North American, Asian, and Indian haze: Similar regional impacts on climate?, *Geophys. Res. Lett.*, *30*(11), 1555, doi:10.1029/2003GL016934.
- Raymond, T., and S. Pandis (2002), Cloud activation of single-component organic aerosol particles, *J. Geophys. Res.*, *107*(D24), 4787, doi:10.1029/2002JD002159.
- Rogge, W. F., L. M. Hildemann, M. A. Mazurek, and G. R. Cass (1996), Mathematical modeling of atmospheric fine particle-associated primary organic compound concentrations, *J. Geophys. Res.*, *101*(D14), 19,379–19,394.
- Ruellan, S., H. Cachier, A. Gaudichet, P. Masclet, and J.-P. Lacaux (1999), Airborne aerosols over central Africa during the Experiment for Regional Sources and Sinks of Oxidants (EXPRESSO), *J. Geophys. Res.*, *104*(D23), 30,627–30,690.
- Sander, R. (1999), Compilation of Henry's law constants for inorganic and organic species of potential importance in environmental chemistry (version 3), Max-Planck Inst. of Chem., Mainz, Germany. (Available at <http://www.mpch-mainz.mpg.de/~sander/res/henry.html>)
- Satsumbayashi, H., H. Kurita, Y. Yokouchi, and H. Ueda (1989), Mono- and di-carboxylic acids under long-range transport of air pollution in central Japan, *Tellus, Ser. B*, *41*, 219–229.
- Saxena, P., and L. M. Hildemann (1996), Water-soluble organics in atmospheric particles: A critical review of the literature and application of thermodynamics to identify candidate compounds, *J. Atmos. Chem.*, *24*, 57–109.
- Schwartz, S. (1986), Mass transport considerations pertinent to aqueous phase reactions of gases in liquid water clouds, in *Chemistry of Multiphase Atmospheric Systems*, NATO ASI Ser., vol. 6, edited by W. Jaeschke, pp. 415–471, Springer-Verlag, New York.
- Sempéré, R., and K. Kawamura (1996), Low molecular weight dicarboxylic acids and related polar compounds in the remote marine rain samples collected from western Pacific, *Atmos. Environ.*, *30*(10/11), 1609–1619.
- Shetter, R. E., L. Cinquini, B. L. Lefler, S. R. Hall, and S. Madronich (2002), Comparison of airborne measured and calculated spectral actinic flux and derived photolysis frequencies during the PEM-Tropics B mission, *J. Geophys. Res.*, *107*, 8234, doi:10.1029/2001JD001320. [printed 108(D2), 2003]
- Shulman, M. L., M. C. Jacobson, R. J. Charlson, R. E. Synovec, and T. E. Young (1996), Dissolution behavior and surface tension effects of organic compounds in nucleating droplets, *Geophys. Res. Lett.*, *23*(3), 277–280.
- Stevens, B., R. L. Walko, W. R. Cotton, and G. Feingold (1996), On elements of the microphysical structure of numerically simulated nonprecipitating stratocumulus, *J. Atmos. Sci.*, *53*, 980–1006.
- Stockwell, W., F. Kirchner, M. Kuhn, and S. Seefeld (1997), A new mechanism for regional atmospheric chemistry modeling, *J. Geophys. Res.*, *102*(D22), 25,847–25,879.
- Stokes, R. H., and R. A. Robinson (1966), Interactions in nonelectrolyte solutions. I. Solute-solvent equilibria, *J. Phys. Chem.*, *70*, 2126–2130.
- Talbot, R. W., B. W. Mosher, B. G. Heikes, D. J. Jacob, J. W. Munger, B. C. Daube, W. C. Keene, J. R. Maben, and R. S. Artz (1995), Carboxylic acids in the rural continental atmosphere over the eastern United States during Shenandoah Cloud and Photochemistry Experiment, *J. Geophys. Res.*, *100*(D5), 9335–9343.
- Volz-Thomas, A., A. Lerner, H. W. Pätz, M. Schultz, D. S. McKenna, R. Schmitt, S. Madronich, and E. P. Röth (1996), Airborne measurements of the photolysis frequency of NO<sub>2</sub>, *J. Geophys. Res.*, *101*(D13), 18,613–18,627.
- Warneck, P. (2003), In-cloud chemistry opens pathway to the formation of oxalic acid in the marine atmosphere, *Atmos. Environ.*, *37*, 2423–2427.
- Whiteaker, J., and K. A. Prather (2003), Hydroxymethanesulfonate as a tracer for fog processing of individual aerosol particles, *Atmos. Environ.*, *37*, 1033–1043.
- Wojcik, G. S., and J. S. Chang (1997), A reevaluation of sulfur budgets, lifetimes, and scavenging ratios for eastern North America, *J. Atmos. Chem.*, *26*, 109–145.
- Zdanovskii, A. B. (1948), New methods of calculating solubilities of electrolytes in multicomponent systems, *Zh. Fiz. Khim.*, *22*, 1475–1485.
- Zhang, Y., S. M. Kreidenweis, and G. Feingold (1999), Stratocumulus processing of gases and cloud condensation nuclei: 2. Chemistry sensitivity analysis, *J. Geophys. Res.*, *104*(D13), 16,061–16,080.
- Zuo, Y., and J. Hoigné (1992), Formation of hydrogen peroxide and depletion of oxalic acid in atmospheric water by photolysis of iron(III)-oxalato-complexes, *Environ. Sci. Technol.*, *26*, 1014–1022.

B. Ervens, Cooperative Institute for Research in the Atmosphere, Colorado State University, Fort Collins, CO 80523, USA. (barbara.ervens@noaa.gov)

G. Feingold, Environmental Technology Laboratory, NOAA, Boulder, CO 80305, USA.

G. J. Frost, Aeronomy Laboratory, NOAA, Boulder, CO 80305, USA.

S. M. Kreidenweis, Atmospheric Science Department, Colorado State University, Fort Collins, CO 80523, USA.